Limited induction of lung-resident memory T cell responses against SARS-CoV-2 by mRNA vaccination

Daan K.J. Pieren[1], Sebastián G. Kuguel[1], Joel Rosado[2], Alba G. Robles[1], Joan Rey-Cano[1], Cristina Mancebo[1], Juliana Esperalba[4], Vicenç Falcó[1], María J. Buzón[1], Meritxell Genescà[1 *]

Affiliations

[1]Infectious Diseases Department, Vall d'Hebron Institut de Recerca (VHIR), Vall d'Hebron Hospital Universitari, Vall d'Hebron Barcelona Hospital Campus, Passeig Vall d'Hebron 119-129, 08035 Barcelona, Spain;

[2]Thoracic Surgery and Lung Transplantation Department, Vall d'Hebron Institut de Recerca (VHIR), Vall d'Hebron Hospital Universitari, Vall d'Hebron Barcelona Hospital Campus, Passeig Vall d'Hebron 119-129, 08035 Barcelona, Spain;

[3]Respiratory Viruses Unit, Microbiology Department, Vall d'Hebron Institut de Recerca (VHIR), Vall d'Hebron Hospital Universitari, Vall d'Hebron Barcelona Hospital Campus, Passeig Vall d'Hebron 119-129,08035 Barcelona, Spain.

*Correspondence: meritxell.genesca@vhir.org (M.G.)

SUMMARY

Resident memory T cells (T_{RM}) present at the respiratory tract may be essential to enhance early SARS-CoV-2 viral clearance, thus limiting viral infection and disease. While long-term antigen (Ag)-specific T_{RM} are detectable beyond 11 months in the lung of convalescent COVID-19 patients after mild and severe infection[1], it is unknown if mRNA vaccination encoding for the SARS-CoV-2 S-protein can induce this frontline protection. We found that the frequency of $CD4^+$ T cells secreting interferon (IFN)γ in response to S-peptides was similar in the lung of mRNA-vaccinated patients compared to convalescent-infected patients. However, in vaccinated patients, lung responses presented less frequently a T_{RM} phenotype compared to convalescent infected individuals and polyfunctional T_{RM} were virtually absent. Thus, a robust and wide T_{RM} response established in convalescent-infected individuals may be advantageous in limiting disease if the virus is not block by initial mechanisms of protection, such as neutralization. Still, mRNA vaccines can induce modest responses within the lung parenchyma potentially contributing to the overall disease control.

MAIN

The COVID-19 pandemic continues, and many countries face multiple resurgences. While vaccines to limit SARS-CoV-2 infection rapidly emerged providing high protection from COVID-19, more insight into the mechanisms of protection induced by available vaccines is still needed. The level of vaccine-induced neutralizing antibodies has been shown to correlate with protection from symptomatic infection; however, predicted antibody-mediated vaccine efficacy declines over time[2]. Moreover, many viral variants of concern (VOC) can significantly evade humoral immunity, yet cellular responses induced by vaccines show strong cross-protection against these variants[3, 4], supporting the idea that cellular responses largely contribute to disease control[5]. In fact, preexisting cross-reactive memory T cells and early Nucleocapsid (N) responses against coronaviruses are associated with protection from SARS-CoV-2 infection[6, 7]. Further, SARS-CoV-2 infection induces robust cellular immunity detectable beyond 10 months after infection in peripheral blood[8], and as T_{RM} in the lung[1], and the number of SARS-CoV-2-specific T_{RM} in the lung correlates with clinical protection[9]. Vaccination against SARS-CoV-2 using BTN162b2 (Pfizer/BioNTech) and mRNA-1273 (Moderna) vaccines has been reported to induce $CD4^+$ and $CD8^+$ T-cell responses in peripheral blood[10, 11]. Moreover, the IFNγ T-cell response to SARS-CoV-2 S-peptides, one of the main antiviral factors measured as a readout, further increased after boosting[11]. However, current studies only address vaccine-induced SARS-CoV-2 specific T-cell responses in peripheral blood and whether mRNA vaccines also elicit SARS-CoV-2-specific long-term T_{RM} cells in the lung remains to be established.

To this end, we determined the presence of SARS-CoV-2-specific $CD4^+$ and $CD8^+$ T cells in 26 paired peripheral blood and lung cross-sectional samples from: I.) uninfected unvaccinated individuals (Ctrl, n=5), II.) unvaccinated long-term SARS-CoV-2 convalescent individuals (Inf, n=9, convalescent for a median of 304 days [183-320 IQR]), III.) uninfected and long-term two-dose vaccinated individuals (Vx2, n=7, a median of 206 days [184-234] after the second dose), and IV.) uninfected and short-term three-dose vaccinated individuals (Vx3, n=5, a median of 52 days [42-54] after the third dose or boost). Patient characteristics are summarized in Extended Table 1. In order to confirm the SARS-CoV-2 status of each patient, we analyzed total immunoglobulin (Ig) or IgG levels against N and Spike (S) proteins respectively, which discriminated Ctrl (negative for N and S), Inf patients (positive for N and S) and vaccinated groups (negative for N and positive for S; Extended Table 1). Furthermore, the viral neutralization titer was determined against the SARS-CoV-2 Omicron variant using a pseudovirus neutralization assay and, as expected[10, 11], a positive correlation between neutralization and S-IgG titers was detected (Spearman r = 0.72, P = 0.0016; Extended Data Fig.1a). In addition to the absence of

neutralization of the Omicron variant in plasma of the Ctrl group, 2 out of 7 patients (28%) in the Inf group and from 1 out of 6 patients (17%) in the Vx2 group failed to neutralize the virus, whereas all patients in the Vx3 group were able to neutralize this variant (Extended Table 1). The fact that we mostly studied elderly patients could certainly determine the overall response and, indeed there was a negative correlation between older age and neutralizing capacity for the Inf group (Spearman r = - 0.88, *P* = 0.01; Extended Data Fig.1b) and the same trend was observed for the Vx2 group (Spearman r = - 0.72, *P* = 0.10; Extended Data Fig.1c). This relationship was less evident between age and S-IgG titers (Extended Data Figs.1d, e), yet examples in larger cohorts exist[10]. Instead, S-IgG titers from all groups negatively correlated with sample timing (Spearman r = -0.61, *P* = 0.010; Extended Data Fig.1f), a correlation that was also observed for total Ig against N in the Inf group (Spearman r = -0.88, *P* = 0.009; Extended Data Fig.1g), which agrees with antibody titers decay[10, 11, 12].

To address cellular immune responses, we stimulated fresh peripheral blood mononuclear cells (PBMC) and lung-derived cellular suspensions with overlapping Membrane (M), N and S peptide pools and determined the intracellular expression of IFNγ, interleukin (IL)-4, and IL-10, along with the degranulation marker CD107a in $CD4^+$ and $CD8^+$ T cells (Extended Data Fig.2a), as previously described[1]. We found detectable circulating IFNγ-secreting Ag-specific $CD4^+$ T cells responding to all proteins in the blood of Inf patients, which was significantly higher compared to the Ctrl, Vx2, and Vx3 groups for M and N peptides (Fig. 1a, b). In contrast, for S peptides, the Inf group only showed higher frequencies of $IFN\gamma^+$ $CD4^+$ T cells compared to the Ctrl group, indicating an increase induced by vaccination in the blood of Vx2 and Vx3 groups. However, only two Vx2 patients showed detectable frequencies of S-specific $CD4^+$ T cells in blood, while recently boosted Vx3 patients displayed an overall increase reaching statistical significance compared to the Ctrl group (Fig. 1b). In contrast to $CD4^+$ T cells, the frequencies of $IFN\gamma^+$ $CD8^+$ T cells detected were minimal for each of the groups against any of the proteins, including for the Vx groups against S peptides (Fig. 1b). Expression of IL-4, IL-10, and CD107a by T cells showed, in general, high variability, limiting the detection of differences (Extended Data Fig. 3). Nonetheless, S-specific degranulating $CD107a^+$ $CD8^+$ T cells were overall more frequent in the Vx2 compared to the Ctrl group (*P* = 0.046; Extended Data Fig. 3). Together, these data indicate that M, N, and S-peptide specific $IFN\gamma^+$ $CD4^+$ T cell responses can be readily detected in blood months after resolving natural SARS-CoV-2 infection and that these responses require a recent mRNA vaccine booster-dose against SARS-CoV-2 to elicit similar frequencies against the S protein in vaccinated individuals.

As reported previously[1], we here found that mild or severe natural infection with SARS-CoV-2 induced robust IFNγ$^+$ CD4$^+$ T cells in the lung against M, N, and S peptides, detectable for up to 12 months after infection (Fig. 2a, b). Interestingly, whereas M and N-specific IFNγ$^+$ CD4$^+$ T-cell frequencies were significantly higher in the Inf group compared to Ctrl or Vx groups, these differences were not observed for S-specific responses (Figs. 2a, b). Vx2 and Vx3 groups showed presence of S-specific IFNγ$^+$ CD4$^+$ T cells in the lung in most patients and its frequency was comparable to levels detected in Inf patients, although statistical significance was no reached compared to the Ctrl group (Fig. 2b). In contrast to CD4$^+$ T cells, CD8$^+$ T cells producing IFNγ after stimulation with M, N, or S peptides was variable within each group and did not result in significant differences between the groups, indicating that natural infection nor vaccination elicit a robust IFNγ positive CD8$^+$ T cell response in the human lung (Fig. 2b). Furthermore, induction of lung anti-SARS-CoV-2-specific T-cell responses involving expression of IL-4, IL-10, and CD107a did not differ between groups (Extended Data Fig. 4a). Of note, in this tissue compartment, we detected negative correlations between patient's age within the Inf group and the frequency of S-specific degranulating CD4$^+$ and CD8$^+$ T cells (Spearman r = - 0.76, P = 0.024 and Spearman r = - 0.77, P = 0.020 respectively, Extended Data Fig. 4b).

When we compared the magnitude of S-specific T cells in paired blood and lung samples, we found increased frequencies of IFNγ$^+$ CD4$^+$ T cells in the lungs of patients from the Inf group compared to blood (P =0.039, Fig. 2c). The same trend was observed for the Vx individuals, which was close to significant if both groups were pooled (P = 0.054). In contrast, the CD8$^+$ T-cell compartment did not show clear differences between these two compartments (Fig. 2c), neither any of the T-cell subsets for any other function, which were highly variable (Extended Data Fig. 5). Together our data shows that S-specific CD4$^+$ T-cell responses are detectable in the lung of uninfected vaccinated patients, indicating that mRNA vaccination against SARS-CoV-2 may elicit tissue-localized protective T-cell responses already after the second mRNA vaccine dose.

Considering the presence of T_{RM} in the respiratory tract might provide a better correlate of protection from disease in SARS-CoV-2 infected individuals[1, 9], we next analyzed expression of CD69 and CD103 by lung SARS-CoV-2-specific CD4$^+$ and CD8$^+$T cells, which we classified as: CD69$^-$ (non-T_{RM}), CD69$^+$ (T_{RM}) and a subset within CD69$^+$ cells expressing CD103$^+$ (T_{RM} CD103$^+$) (Fig. 3a, Extended Data Fig. 2b for gating strategy). Of note, CD69$^+$T cells showed down-regulation of T-bet in all groups (Extended Data Fig. 2b), which has been associated to tissue residency[1]. S-specific CD4$^+$ T cells from the Inf group showed higher frequencies of IFNγ$^+$ cells within the CD69$^+$ and CD103$^+$ T_{RM} phenotypes (Fig. 3a, b), with statistical significance reached for the overall CD69$^+$ T_{RM} fraction compared to the non-T_{RM} fraction. Furthermore, while no

significant differences were detected for CD103$^+$ T_{RM} cells against S-peptides in any of the groups, a trend was observed for CD4$^+$ T-cell responses to M peptides and statistical significance was reached for CD8$^+$ T cells against N peptides compared to the non-T_{RM} fraction in the Inf group (Extended Data Fig. 6a, b). Of note, a negative correlation was observed between IFNγ-secreting S-specific CD8$^+$ CD103$^+$ T_{RM} cells and sample timing (Spearman r = - 0.82, *P* = 0.019 Extended Data Fig. 6c). Similar to the Inf group, some patients in the Vx2 and Vx3 groups showed presence of S-specific T_{RM} with or without CD103 expression in their lungs (Figs. 3a, b). However, this response was highly heterogeneous and not statistically significant. These findings indicate that mRNA vaccination against SARS-CoV-2 can induce S-specific T_{RM} in some, but not all individuals and may also last long term after the second vaccination.

To better gain insight into the overall S-specific response by each group, including all functions and considering lung-T_{RM} phenotypes, we represented S-specific CD4$^+$ and CD8$^+$ T cell subsets as donut charts displaying the mean frequency of responses including all individuals (responders and non-responders, Fig. 4, b). This way, a dominance of IFNγ-secreting CD4$^+$ T cells was particularly associated to the two T_{RM} phenotypes in the Inf and, to a lesser extent, in the Vx2 patients (Fig. 4a). Further, S-specific responses within non-T_{RM} and blood CD4$^+$ T cells were functionally similar and in general dominated by IFNγ and IL-4 secretion (Fig. 4a). In contrast, degranulation characterized the majority of lung S-specific CD8$^+$ T cells from Inf individuals (Fig. 4b), which correlated negatively with older age for the T_{RM} fractions (Spearman r = - 0.88, *P* = 0.006 for both CD103 positive and negative, Extended Data Fig. 6d). Degranulation was also the major function in blood from the two Vx groups (Fig. 4b). Last, in general, CD8$^+$ T-cell responses considering all functions were of higher magnitude in long-term Vx2 individuals, reaching statistical significance for blood responses in comparison to the Ctrl group, as shown in the adjoin graph on the right (Fig. 4b).

We previously detected a low but consistent polyfunctional IFNγ$^+$CD107a$^+$ T-cell response mostly associated to the T_{RM} fraction in convalescent infected patients[1]. We therefore investigated whether mRNA vaccination against SARS-CoV-2 would also induce S-specific polyfunctional responses in both compartments (Figs. 5a, b). Indeed, increased frequencies of polyfunctional IFNγ$^+$CD107a$^+$ CD4$^+$ T cells were detected in blood from the Inf group against N peptides compared to the Ctrl group, but not against M- and S-peptides. Interestingly, a trend towards higher frequencies of S-specific polyfunctional CD4$^+$ T cells was observed for the Vx3 group (Fig. 5a). Likewise, circulating polyfunctional S-specific CD8$^+$ T cells were enhanced in Vx2 individuals compared to Ctrl group (Fig. 5a). In fact, if Vx groups were pooled to increase sample size, then both CD4$^+$ and CD8$^+$ T cells reached significance compared to Ctrl samples (*P* = 0.037 for CD4$^+$

and $P = 0.024$ for $CD8^+$). In addition, the frequency of polyfunctional $IFN\gamma^+CD107a^+$ cells present in total $CD4^+$ and $CD8^+$ T cells in the lung were only consistently increased in the Inf group against N peptides compared to the Ctrl and Vx3 groups (Fig. 5b). Nevertheless, while a high degree of variability was observed among vaccinated patients, polyfunctional S-specific T cells were detected in some individuals (Fig. 5b). Strikingly, S-specific $CD4^+$ polyfunctional $CD103^+$ T_{RM} cells were virtually absent in the Vx2 and Vx3 groups, while being frequently present in the lungs of patients from the Inf group (Extended data Fig. 7). Furthermore, the frequency of S-specific polyfunctional $CD4^+$ T cells in the $CD69^+$ T_{RM} cells was higher in the Inf group compared to the Ctrl and Vx2 groups (Extended data Fig. 7). Together, these data indicate that both short- and long-term vaccination do not induce S-specific $IFN\gamma^+CD107a^+$ $CD103^+$ T_{RM} cells in the lung, which may contribute to antiviral activity.

Last, considering the uniqueness of analyzing immune responses in paired blood and lung parenchyma samples and recent studies detailing changes in T cell responses in infected individuals already vaccinated and vice versa[13], we highlight two patients that were discarded due to not fitting inclusion criteria, yet bring interesting data to the study. HL174 was a patient in their fifties who received the third mRNA-1273 vaccine boost and, five days after, tested positive by PCR. We analyzed paired tissue samples 30 days after the boost/infection event (Extended Data Fig. 8a). This patient had a neutralization titer of 1740 IU/mL against omicron, and had detectable IgG and Ig titers against S and N proteins (>800 AU/mL and 1.23 index, respectively). When comparing T-cell responses from blood and lung tissue, a much higher IFNγ-response was observed in the lung, in particular against the N protein, which already contained responding cells with a T_{RM} phenotype (Extended Data Fig. 8b, c). In contrast, in blood, degranulation was enhanced mostly against S but also M protein and some proportion of IL-10 secretion was detected against all proteins (Extended Data Fig. 8b).

On the other hand, patient HL162, who was in their early seventies, was first infected presenting a mild COVID-19 and, several months after, received three doses of the mRNA-1273 vaccine. In this case, we obtained samples 3.7 months after infection and another one 1.3 months after the third dose (due to a second intervention for a lung carcinoma), which corresponded to a year after initial infection, as shown (Extended Data Fig. 9a). Neither of these two time points showed neutralization titers against omicron and the titers of IgG, instead of increasing after triple vaccination, decreased from 156 to 0 index for the N protein and from 306.54 to 13.85 AU/mL for S protein. The comparison of the tissue compartments after infection and after triple vaccination evidenced a concomitant strong decrease in T-cell responses in blood and tissue (Extended Data Figs. 9b, c, and Extended Data Fig. 10a, b). However, IFNγ-secreting SARS-CoV-2 T cells against

M and N proteins in the lung were better preserved from the original infection one year later than were responses against the S protein enhanced due to vaccination (Extended Data Fig. 9b, c, and Extended Data Fig. 10a, b). Thus, while the lower respiratory tract compartment more faithfully represented T_{RM} responses established already during the infection event one year earlier, responses in blood mostly vanished.

Comprehensive studies comparing the magnitude and duration of the T cell responses indicate similar magnitude after dual vaccination and after natural SARS-CoV-2 infection[5, 11, 13]. However, these results may not hold if we consider that the magnitude, the functional profile and even the duration of these responses in blood may not faithfully reflect responses in the respiratory tract[1, 7, 9, 14]. In fact, the individual comparison between these two compartments among the S-responding T cells from the different groups showed higher magnitude in the lung than in the blood, but also a different profile. A key difference, and the main driver of our study, was the establishment of long-term protection potentially mediated by T_{RM} after vaccination, since longevity of SARS-CoV-2 T cell responses remains a critical question[7]. In principle, T_{RM} are established by mucosal infection since Ag together with local signals promote the recruitment and establishment of this memory response. In this sense, intramuscular vaccination with an adenovector vaccine in mice did not induce SARS-CoV-2-specific T_{RM} in their lungs[15]. Thus, to induce potent resident immunity, vaccine strategies may need to either use live-attenuated Ag or employ mucosal routes. Consequently, the absence of vaccine induced S-specific T_{RM} could be expected in infection-naïve individuals. Still, recent data shows that a secretory IgA response was induced in ~30% of participants after two doses of a SARS-CoV-2 mRNA vaccine which, in addition, may play an important role in protection against infection[14]. While we detected S-specific $IFN\gamma^+$ $CD4^+$ T cell responses in the lung of vaccinated individuals, the proportion of these cells in the T_{RM} phenotype was modest, in particular if considering CD103 expression. Further, the presence of polyfunctional $IFN\gamma^+CD107a^+CD4^+CD103^+T_{RM}$ appeared to be restricted to the lungs of convalescent-infected patients only. Yet, lung S-specific $CD8^+$ T_{RM} presented similar overall frequencies in vaccinated individuals when considering all functions. In fact, overall $CD8^+$ T cell response, which was in general low and dominated by degranulation, appeared enhanced in some but not all vaccinated patients. Considering the putative protective role of $CD8^+$ T cells observed in animal models[16], our results for these vaccinated individuals are certainly encouraging.

Another difference in the comparison of the cellular immunity between SARS-CoV-2-infected convalescent and uninfected-vaccinated individuals is the broader and, potentially stronger, response induced by symptomatic infection. This is partially manifested by the fact that,

when comparing the overall magnitude, responses against M and N peptides are frequently higher than S peptides[1, 17, 18 19]. Of note, disease severity may impact both, the magnitude and function of the T cell response against the different proteins[1, 20, 21]. In addition, among other factors, age also influences the magnitude and duration of immune responses in distinct tissue compartments, even the establishment of T_{RM}[22], a factor that influenced the frequency of degranulation in the lung of our Inf patients, including within the T_{RM} fraction. Yet advanced age will also limit the immune response to vaccination[23]. On the other hand, we have observed that different proteins induce different functional profiles during acute infection, which may influence disease control[1]. Responses against the N protein seem to more consistently induce polyfunctional antiviral T cells and these responses may be more conserved among other coronaviruses[1, 6, 24, 25]. Instead, S-specific immune responses may better support B cell and antibody generation via follicular helper T cells, instrumental for limiting infection[1, 5]. Thus, another conclusion would be highlighting the interest of including other proteins beyond the spike such as N sequences, which has been suggested before[1, 6, 19, 25, 26]. Last, in terms of duration, our study lacks longitudinal data to assess the dynamics in the different compartments, yet it is assumed that T_{RM} phenotypes will contribute to long-term persistence[1, 7, 16]. In fact, the only patient for which we had longitudinal sampling after infection and after the third vaccine boost (extended Fig. 9) demonstrated that even if vaccination fails to induce a systemic antibody response, a low frequency SARS-CoV-2 T cell response directed to proteins from the original infection remains exclusively detectable in the lung as T_{RM} one year after.

We acknowledge that our study has several limitations, including the small sample size for the different groups. In addition, we addressed T cell immune responses in older and mostly oncologic patients, which may overall underestimate immune responses in all groups. Whereas the fact that the Inf group consisted of patients recovered from mild or severe disease, even if age and underlying conditions were similar to the other groups, may have skewed frequencies of SARS-CoV-2-specific T cells towards the higher end. Still, considering their age and condition, any of these patients with a new infection would most likely develop a more serious COVID-19 event compared to the general population. In addition, the boosted Vx3 group was sampled short term comparing to the Vx2 group, but enhancement of T cell responses would be better detected 5-10 days after boosting[10, 11] (which was a less likely time for scheduling surgery). Still it was enough to suggest that there was no major enhancement of long-term durable T cell response in the lung by a third boost. Further, we did not assess the contribution of T cells targeting mutation regions to the total spike since we aimed to compare the strength and function of vaccinated and naturally infected patients (these last group obtained during the first wave). However, the overall

contribution of T cell responses to mutational regions/total spike responses has been reported to be low[13, 27]. Last, low percentages of SARS-CoV-2 specific $CD8^+$ T cells may be due to the use of 15-mer peptides, which are less optimal than 9/10-mer peptides for HLA class I binding[4], although this is debatable[21].

Overall, our results contribute to the understanding of disease protection mediated by current mRNA vaccines. While our data indicates a more robust and broader cellular response in convalescent patients, S-specific T cells can be detected in the lung of vaccinated individuals to similar overall levels 8 months after immunization, highlighting the durability of this immune arm. Further, while we detected increased levels of $IFN\gamma^+$ T cell responses in blood after the third dose, limited benefit of boosting towards the enhancement of T cell responses in the lung was evidenced by our data. However, elderly people not responding to vaccination have been shown to benefit from a third dose[23] and there is an obvious benefit of boosting to provide a higher degree of antibody-mediated protection from infection in the context of high incidence of VOC[2]. Still, if virus neutralization is unable to completely block infection, a more robust and wider T_{RM} response established in the lung of convalescent-infected individuals may have more chances of limiting disease. The inclusion of other protein fragments such as nucleocapsid peptides[1, 6, 19, 25, 26] in combination with mucosal routes[28] will likely contribute to the establishment of optimal memory T cells in future vaccine strategies.

METHODS

Ethics statement

This study was performed in accordance with the Declaration of Helsinki and approved by the corresponding Institutional Review Board (PR(AG)212/2020) of the Vall d'Hebron University Hospital (HUVH), Barcelona, Spain. Written informed consent was provided by all patients recruited to this study.

Subject recruitment and sample collection

Patients undergoing lung resection for various reasons at the HUVH were recruited through the Thoracic Surgery Service and invited to participate. Initially, a total of 32 patients, from whom paired blood samples and lung biopsies were collected were assayed. However, based on vaccination and/or infection status of the recruited patients, 26 (+2: HL174 and HL162) patients were finally included. Extended data Table 1 summarizes relevant information from included patients. For all participants, whole blood was collected with EDTA anticoagulant. Plasma was collected and stored at −80 °C (except for 4 patients distributed among the different groups, as

indicated in Extended Data Table 1, for which this sample was not available) and PBMCs were isolated via Ficoll–Paque separation and processed immediately for stimulation assays.

Phenotyping and Intracellular Cytokine Staining of lung biopsies

Immediately following surgery, healthy areas from patients undergoing lung resection were collected in antibiotic-containing RPMI 1640 medium and processed as published[1]. Briefly, 8-mm^3 dissected blocks were first enzymatically digested with 5 mg/ml collagenase IV (Gibco) and 100µg/ml of DNase I (Roche) for 30 min at 37 ºC and 400 rpm and, then, mechanically digested with a pestle. The resulting cellular suspension was first filtered through a 70µm pore size cell strainer and then filtered through a 30µm pore size cell strainer (Labclinics). After washing with PBS, cells were stimulated in a 96-well round-bottom plate for 16 to 18 hours at 37°C with 1µg/mL of SARS-CoV-2 peptides (PepTivator SARS-CoV-2 M, N or S, Miltenyi Biotec) in the presence of 3.3µL/mL α-CD28/CD49d (clones L293 and L25), 0.55µL/mL Brefeldin A, 0.385µL/mL Monensin and 5 µL/100µL anti-CD107a-PE-Cy5 (all from BD Biosciences). For each patient, a negative control, cells treated with medium, and positive control, cells incubated in the presence of 0.4nM PMA and 20µM Ionomycin, were included. Next day, cellular suspensions were stained with Live/Dead Aqua (Invitrogen) and anti-CD103 (FITC, Biolegend), anti-CD69 (PE-CF594, BD Biosciences), anti-CD40 (APC-Cy7, Biolegend), anti-CD8 (APC, BD Biosciences), anti-CD3 (BV650, BD Biosciences) and anti-CD45 (BV605, BD Biosciences) antibodies. Cells were subsequently fixed and permeabilized using the FoxP3 Fix/Perm kit (BD Biosciences) and stained with anti-IL-4 (PE-Cy7, eBioscience), anti-IL-10 (PE, BD Biosciences), anti-T-bet (BV421, Biolegend) and anti-IFNγ (AF700, Invitrogen) antibodies. After fixation with PBS 2% PFA, cells were acquired in a BD LSR Fortessa flow cytometer (Cytomics Platform, High Technology Unit, Vall d'Hebron Institut de Recerca).

Phenotyping and Intracellular Cytokine Staining in blood

Freshly isolated PBMCs were labelled for CCR7 (PE-CF594, BD Biosciences) and CXCR3 (BV650, BD Biosciences) for 30 min at 37ºC. After washing with PBS, PBMCs were stimulated in a 96-well round-bottom plate for 16 to 18 hours at 37°C with 1µg/mL of SARS-CoV-2 peptides together with the same concentration of Brefeldin A, Monensin, α-CD28/CD49d and CD107a-PE-Cy5, as stated for the lung suspension above and published before[1]. For each patient, a negative control and a positive control were also included. After stimulation, cells were washed twice with PBS and stained with Aqua LIVE/DEAD fixable dead cell stain kit (Invitrogen). Cell surface antibody staining included anti-CD3 (Per-CP), anti-CD4 (BV605) and anti-CD56 (FITC) (all from

BD Biosciences). Cells were subsequently fixed and permeabilized using the Cytofix/Cytoperm kit (BD Biosciences) and stained with anti-Caspase-3 (AF647, BD Biosciences), anti-Bcl-2 (BV421, Biolegend), anti-IL-4 (PE-Cy7, eBioscience), anti-IL-10 (PE, BD Biosciences) and anti-IFNg (AF700, Invitrogen) for 30 mins. Cells were then fixed with PBS 2% PFA and acquired in a BD LSR Fortessa flow cytometer.

SARS-CoV-2 serology

The serological status of patients included in this study was determined in serum samples using two commercial chemiluminescence immunoassays (CLIA) targeting specific SARS-CoV-2 antibodies: (1) Elecsys Anti-SARS-CoV-2 (Roche Diagnostics, Mannheim, Germany) was performed on the Cobas 8800 system (Roche Diagnostics, Basel, Switzerland) for the determination of total antibodies (including IgG, IgM, and IgA) against nucleocapsid (N) SARS-CoV-2 protein; and (2) Liaison SARS-CoV-2 TrimericS IgG (DiaSorin, Stillwater, MN) was performed on the LIAISON XL Analyzer (DiaSorin, Saluggia, Italy) for the determination of IgG antibodies against the spike (S) glycoprotein.

Pseudovirus neutralization assay

The spike of the Omicron SARS-CoV-2 was generated (GeneArt Gene Synthesis, ThermoFisher Scientific) from the plasmid containing the D614G mutation with a deletion of 19 amino acids, which was modified to include the mutations specific for this VOC (A67V, Δ69-70, T95I, G142D/Δ143-145, Δ211/L212I, ins214EPE, G339D, S371L, S373P, S375F, K417N, N440K, G446S, S477N, T478K, E484A, Q493R, G496S, Q498R, N501Y, Y505H, T547K, D614G, H655Y, N679K, P681H, N764K, D796Y, N856K, Q954H, N969K, L981F) (kindly provided by Drs. J. Blanco and B. Trinite). Pseudotyped viral stocks of VSV*ΔG(Luc)-S were generated following the protocol described in[29]. Briefly, 293T cells were transfected with 3µg of the omicron plasmid (pcDNA3.1 omicron). Next day, cells were infected with a VSV-G-Luc virus (MOI=1) for 2h and washed twice with warm PBS. To neutralize contaminating VSV*ΔG(Luc)-G particles cells were incubated overnight in media containing 10% of the supernatant from the I1 hybridoma (ATCC CRL-2700), containing anti-VSV-G antibodies. Next day, viral particles were harvested and titrated in VeroE6 cells by enzyme luminescence assay (Britelite plus kit; PerkinElmer). For the neutralization assays, VeroE6 cells were seeded in 96-well white, flat-bottom plates (Thermo Scientific) at 30,000 cells/well. Plasma samples were heat-inactivated and diluted four-fold towards a concentration of 1/32 of the initial sample. Diluted plasma samples were then incubated with pseudotyped virus (VSV*ΔG(Luc)-$S^{omicron}$) with titers of approximately $1x10^6$ – $5x10^5$ RLUs/ml

of luciferase activity - in a 96 well-plate flat bottom for 1 hour at 37°C, 5% CO_2. Next, 30,000 Vero E6 cells were added to each well and incubated at 37°C, 5% CO_2 for 20-24 hours. Then, viral entry was measured by the expression of luciferase. Cells were incubated with Britelite plus reagent (Britelite plus kit; PerkinElmer) and then transferred to an opaque black plate. Luminescence was immediately recorded by a luminescence plate reader (LUMIstar Omega). Viral neutralization was calculated as the reciprocal plasma dilution (ID50) resulting in a 50% reduction in relative light units. If no neutralization was observed, an arbitrary titer value of 16 (half of the limit of detection [LOD]) was reported.

Statistical analyses

Flow cytometry data was analyzed using FlowJo v10.7.1 software (TreeStar). Data and statistical analyses were performed using Prism 8.0 (GraphPad Software, La Jolla, CA, USA). Data shown in bar graphs were expressed as median and Interquartile range (IQR), unless stated otherwise. Correlation analyses were performed using non-parametric Spearman rank correlation. Kruskal-Wallis rank-sum test with Dunn's post-hoc test was used for multiple comparisons. Friedmann test with Dunn's post-hoc test was applied for paired comparisons. A *P* value <0.05 was considered statistically significant. Antigen-specific T-cell data was calculated as the net frequency, where the individual percentage of expression for a given molecule in the control condition (vehicle) was subtracted from the corresponding SARS-CoV-2-peptide stimulated conditions.

ACKNOWLEDGMENTS

We would like to thank all the patients who participated in the study and Drs. Julià Blanco and Benjamin Trinite for providing the plasmid encoding the omicron spike. This work was supported by grants from Fundació La Marató TV3 (201814-10 FMTV3 and 202112-30 FMTV3), from the Health department of the Government of Catalonia (DGRIS 1_5), and the Spanish AIDS network Red Temática Cooperativa de Investigación en SIDA (RD16/0025/0007). M.J.B is supported by the Miguel Servet program funded by the Spanish Health Institute Carlos III (CP17/00179). The funders had no role in study design, data collection and analysis, the decision to publish, or preparation of the manuscript.

AUTHOR CONTRIBUTIONS

Conceptualization, M.G.; Patient Recruitment and Sample Collection, J.R., V.F.; Methodology, DKJ.P., SG.K., A.G.R., J.R-C, C.M., J.E.; Investigation, DKJ.P., SG.K., A.G.R., J.E.; Formal

Analysis, DKJ.P., A.G.R., M.J.B. and M.G.; Writing-Original Draft, DKJ.P. and M.G; Writing-Review & Editing, all authors; Funding Acquisition, M.G.; Supervision, M.G.

DECLARATION OF CONFLICT OF INTEREST

The authors declare no competing interest.

DATA AVAILABILITY

The authors declare that the data supporting the findings of this study are available within the paper and its supplementary information files.

REFERENCES

1. Grau-Exposito J, Sanchez-Gaona N, Massana N, Suppi M, Astorga-Gamaza A, Perea D*, et al.* Peripheral and lung resident memory T cell responses against SARS-CoV-2. *Nature communications* 2021, **12**(1)**:** 3010.

2. Cromer D, Steain M, Reynaldi A, Schlub TE, Wheatley AK, Juno JA*, et al.* Neutralising antibody titres as predictors of protection against SARS-CoV-2 variants and the impact of boosting: a meta-analysis. *The Lancet Microbe* 2022, **3**(1)**:** e52-e61.

3. Geers D, Shamier MC, Bogers S, den Hartog G, Gommers L, Nieuwkoop NN*, et al.* SARS-CoV-2 variants of concern partially escape humoral but not T-cell responses in COVID-19 convalescent donors and vaccinees. *Science immunology* 2021, **6**(59).

4. Keeton R, Tincho MB, Ngomti A, Baguma R, Benede N, Suzuki A*, et al.* T cell responses to SARS-CoV-2 spike cross-recognize Omicron. *Nature* 2022, **603**(7901)**:** 488-492.

5. Moss P. The T cell immune response against SARS-CoV-2. *Nat Immunol* 2022, **23**(2)**:** 186-193.

6. Kundu R, Narean JS, Wang L, Fenn J, Pillay T, Fernandez ND*, et al.* Cross-reactive memory T cells associate with protection against SARS-CoV-2 infection in COVID-19 contacts. *Nature communications* 2022, **13**(1)**:** 80.

7. Niessl J, Sekine T, Buggert M. T cell immunity to SARS-CoV-2. *Seminars in immunology* 2021, **55:** 101505.

8. Jung JH, Rha MS, Sa M, Choi HK, Jeon JH, Seok H*, et al.* SARS-CoV-2-specific T cell memory is sustained in COVID-19 convalescent patients for 10 months with successful development of stem cell-like memory T cells. *Nature communications* 2021, **12**(1)**:** 4043.

9. Szabo PA, Dogra P, Gray JI, Wells SB, Connors TJ, Weisberg SP*, et al.* Longitudinal profiling of respiratory and systemic immune responses reveals myeloid cell-driven lung inflammation in severe COVID-19. *Immunity* 2021, **54**(4)**:** 797-814 e796.

10. Goel RR, Painter MM, Apostolidis SA, Mathew D, Meng W, Rosenfeld AM*, et al.* mRNA vaccines induce durable immune memory to SARS-CoV-2 and variants of concern. *Science* 2021, **374**(6572)**:** abm0829.

11. Zhang Z, Mateus J, Coelho CH, Dan JM, Moderbacher CR, Galvez RI*, et al.* Humoral and cellular immune memory to four COVID-19 vaccines. *bioRxiv : the preprint server for biology* 2022.

12. Ortega N, Ribes M, Vidal M, Rubio R, Aguilar R, Williams S*, et al.* Seven-month kinetics of SARS-CoV-2 antibodies and role of pre-existing antibodies to human coronaviruses. *Nature communications* 2021, **12**(1)**:** 4740.

13. Minervina AA, Pogorelyy MV, Kirk AM, Crawford JC, Allen EK, Chou CH, *et al.* SARS-CoV-2 antigen exposure history shapes phenotypes and specificity of memory CD8 T cells. *medRxiv : the preprint server for health sciences* 2022.

14. Sheikh-Mohamed S, Isho B, Chao GYC, Zuo M, Cohen C, Lustig Y, *et al.* Systemic and mucosal IgA responses are variably induced in response to SARS-CoV-2 mRNA vaccination and are associated with protection against subsequent infection. *Mucosal immunology* 2022.

15. Hassan AO, Kafai NM, Dmitriev IP, Fox JM, Smith BK, Harvey IB, *et al.* A Single-Dose Intranasal ChAd Vaccine Protects Upper and Lower Respiratory Tracts against SARS-CoV-2. *Cell* 2020, **183**(1)**:** 169-184 e113.

16. Channappanavar R, Zhao J, Perlman S. T cell-mediated immune response to respiratory coronaviruses. *Immunologic research* 2014, **59**(1-3)**:** 118-128.

17. Le Bert N, Clapham HE, Tan AT, Chia WN, Tham CYL, Lim JM, *et al.* Highly functional virus-specific cellular immune response in asymptomatic SARS-CoV-2 infection. *The Journal of experimental medicine* 2021, **218**(5).

18. Grifoni A, Weiskopf D, Ramirez SI, Mateus J, Dan JM, Moderbacher CR, *et al.* Targets of T Cell Responses to SARS-CoV-2 Coronavirus in Humans with COVID-19 Disease and Unexposed Individuals. *Cell* 2020, **181**(7)**:** 1489-1501 e1415.

19. Taus E, Hofmann C, Ibarrondo FJ, Hausner MA, Fulcher JA, Krogstad P, *et al.* Dominant CD8(+) T Cell Nucleocapsid Targeting in SARS-CoV-2 Infection and Broad Spike Targeting From Vaccination. *Front Immunol* 2022, **13:** 835830.

20. Demaret J, Lefevre G, Vuotto F, Trauet J, Duhamel A, Labreuche J, *et al.* Severe SARS-CoV-2 patients develop a higher specific T-cell response. *Clinical & translational immunology* 2020, **9**(12)**:** e1217.

21. Thieme CJ, Anft M, Paniskaki K, Blazquez-Navarro A, Doevelaar A, Seibert FS, *et al.* Robust T Cell Response Toward Spike, Membrane, and Nucleocapsid SARS-CoV-2 Proteins Is Not Associated with Recovery in Critical COVID-19 Patients. *Cell reports Medicine* 2020, **1**(6)**:** 100092.

22. Poon MML, Byington E, Meng W, Kubota M, Matsumoto R, Grifoni A, *et al.* Heterogeneity of human anti-viral immunity shaped by virus, tissue, age, and sex. *Cell reports* 2021, **37**(9)**:** 110071.

23. Romero-Olmedo AJ, Schulz AR, Hochstatter S, Das Gupta D, Virta I, Hirseland H, *et al.* Induction of robust cellular and humoral immunity against SARS-CoV-2 after a third dose of BNT162b2 vaccine in previously unresponsive older adults. *Nature microbiology* 2022, **7**(2)**:** 195-199.

24. Matchett WE, Joag V, Stolley JM, Shepherd FK, Quarnstrom CF, Mickelson CK, *et al.* Cutting Edge: Nucleocapsid Vaccine Elicits Spike-Independent SARS-CoV-2 Protective Immunity. *Journal of immunology* 2021, **207**(2)**:** 376-379.

25. Peng Y, Felce SL, Dong D, Penkava F, Mentzer AJ, Yao X, *et al.* An immunodominant NP105-113-B*07:02 cytotoxic T cell response controls viral replication and is associated with less severe COVID-19 disease. *Nat Immunol* 2022, **23**(1)**:** 50-61.

26. Mazzoni A, Di Lauria N, Maggi L, Salvati L, Vanni A, Capone M, *et al.* First-dose mRNA vaccination is sufficient to reactivate immunological memory to SARS-CoV-2 in subjects who have recovered from COVID-19. *The Journal of clinical investigation* 2021, **131**(12).

27. Skelly DT, Harding AC, Gilbert-Jaramillo J, Knight ML, Longet S, Brown A, *et al.* Two doses of SARS-CoV-2 vaccination induce robust immune responses to emerging SARS-CoV-2 variants of concern. *Nature communications* 2021, **12**(1)**:** 5061.

28. Mao T, Israelow B, Suberi A, Zhou L, Reschke M, Pena-Hernandez MA, *et al.* Unadjuvanted intranasal spike vaccine booster elicits robust protective mucosal immunity against sarbecoviruses. *bioRxiv : the preprint server for biology* 2022.

29. Grau-Exposito J, Perea D, Suppi M, Massana N, Vergara A, Soler MJ*, et al.* Evaluation of SARS-CoV-2 entry, inflammation and new therapeutics in human lung tissue cells. *PLoS pathogens* 2022, **18**(1)**:** e1010171.

FIGURE LEGENDS

Fig. 1. SARS-CoV-2-specific T-cell responses in peripheral blood from convalescent and vaccinated patients. (**a**) Representative flow-cytometry plots showing $CD4^+$ T cells expressing CD107a and IFNγ after exposure of whole PBMCs to S-peptide pools or left unstimulated for each of the four groups included in this study (complete gating strategy is shown in Extended Data Fig. 2a). (**b**) Comparison of the net frequency (background subtracted) of $IFN\gamma^+$ cells within $CD4^+$ (upper) and $CD8^+$ (lower) T-cell subsets after stimulation of PBMCs with any of the three viral peptide pools (membrane (M), nucleocapsid (N) and spike (S) peptides). Data are shown as median ± IQR, where each dot represents an individual patient for each group (Ctrl, control, n=5; Inf, convalescent infected, n=9; Vx2, vaccine 2 doses, n=7 and Vx3, vaccine 3 doses, n=5). Statistical significance was determined by Kruskal-Wallis test (with Dunn's post-test).

Fig. 2. SARS-CoV-2-specific lung T-cell responses from convalescent and vaccinated patients and comparison between tissue compartments. (**a**) Representative flow-cytometry plots showing $CD4^+$ T cells expressing CD107a and IFNγ after exposure of single-cell suspensions of lung tissue to S-peptide pools or left unstimulated for each of the four groups included in this study (complete gating strategy is shown in Extended Data Fig. 2b). (**b**) Comparison of the net frequency (background subtracted) of $IFN\gamma^+$ cells within $CD4^+$ (upper) and $CD8^+$ (lower) T-cell subsets after exposure of lung single-cell suspensions to any of the three viral peptide pools (membrane (M), nucleocapsid (N) and spike (S) peptides). (**c**) Comparison of the net frequency of $IFN\gamma^+$ cells within $CD4^+$ (left) and $CD8^+$ (right) T-cell subsets in paired blood and lung samples of each group after exposure to S-peptide pools. Data in bar graphs are shown as median ± IQR, where each dot represents an individual patient for each group (Ctrl, control, n=5; Inf, convalescent infected, n=9; Vx2, vaccine 2 doses, n=7 and Vx3, vaccine 3 doses, n=5). Statistical significance was determined by (**b**) Kruskal-Wallis test (with Dunn´s post-test) or (**c**) Friedmann test (with Dunn´s post-test).

Fig. 3. Frequency of Spike-specific T_{RM} cells in the lung. (**a**) Representative flow-cytometry plots showing three subsets of $CD4^+$ T cells present in the lung: $CD69^-$ non-T_{RM}, $CD69^+$ T_{RM}, and $CD69^+CD103^+$ T_{RM} cells expressing CD107a and IFNγ after exposure of single-cell suspensions of lung tissue to S-peptide pools or left unstimulated for an Inf and a Vx2 patients. (**b**) Comparison of the net frequency of S-specific $IFN\gamma^+$ cells within the three (non-) T_{RM} cell subsets present in

the lung for each group. Data in bar graphs are shown as median ± IQR, where each dot represents an individual patient for each group (Ctrl, control, n=5; Inf, convalescent infected, n=8; Vx2, vaccine 2 doses, n=7 and Vx3, vaccine 3 doses, n=4). Statistical significance was determined by Friedmann test (with Dunn´s post-test) for the difference between the cellular subsets within each patient group.

Fig. 4. Overall functional T-cell response of lung and blood compartments. (**a, b**) Donut charts displaying the net contribution of each functional marker (IFNγ, CD107a, IL-4, and IL-10) to the overall S-specific $CD4^+$ (**a**) and $CD8^+$ (**b**) T-cell response within the lung resident and non-resident T-cell subsets and in peripheral blood for each of the individual patient groups. Data represent the mean value of the net frequency of each function within the patient group, including both responders and non-responders. The frequency shown inside each donut chart represents the accumulated mean response of all functions. Bar charts on the right show the mean of the total frequency considering all functions per group (mean ± SD). Statistical significance was determined by Kruskal-Wallis test (with Dunn´s post-test) for the difference between each group. * $P < 0.05$.

Fig. 5. Polyfunctional $CD4^+$ and $CD8^+$ T-cell responses in blood and lung of convalescent and vaccinated patients. (**a, b**) Comparison of the net frequency of polyfunctional $CD107a^+$ $IFN\gamma^+$ cells within $CD4^+$ and $CD8^+$ T-cell subsets for each of the four groups after exposure of PBMCs (**a**) or single-cell suspensions of lung tissue (**b**) to any of the three viral peptide pools (membrane (M), nucleocapsid (N) and spike (S) peptides). Data in bar graphs are shown as median ± IQR, where each dot represents an individual patient for each group (Ctrl, control, n=5; Inf, convalescent infected, n=9; Vx2, vaccine 2 doses, n=7 and Vx3, vaccine 3 doses, n=5). Statistical significance was determined by was determined using Kruskal-Wallis test (with Dunn´s post-test).

EXTENDED DATA LEGENDS

Extended Data Fig. 1. Correlation between SARS-CoV-2-specific antibodies, neutralizing capacity, age, and sampling time. Graphs show the relationship between: (**a**) S-specific IgG antibodies (AU/mL) in plasma and SARS-CoV-2 neutralization titer for each group (Inf, convalescent infected, n=7; Vx2, vaccine 2 doses, n=6 and Vx3, vaccine 3 doses, n=4); (**b, c**) SARS-CoV-2 neutralization titer and age of Inf patients (**b**) and Vx2 patients (**c**); (**d, e**) S-specific IgG antibodies (AU/mL) and age of Inf patients (**d**) and Vx2 patients (**e**); (**f**) S-specific IgG antibodies (AU/mL) in all groups and day of sampling after infection or vaccination; and (**e**) N-specific Ig antibodies (index) in Inf patients and day of sampling after infection. Correlations (*r* and *P* values) were assessed by Spearman test.

Extended Data Fig. 2. Gating strategy for the analysis of T cells present in peripheral blood and lung tissue. (**a, b**) Representative flow-cytometry plots showing the gating strategy towards the identification of $CD4^+$ and $CD8^+$ T cells within PMBC (**a**) and lung tissue (**b**) samples. $CD4^+$ and $CD8^+$ T-cell subsets in PBMCs were identified by gating of time (to exclude disturbances in flow measurements), followed by gating of total lymphocytes, single cells, and live cells. $CD4^+$ and $CD8^+$ T-cell subsets in lung tissue were identified by gating of time, live $CD45^+$ cells, single cells, and lymphocytes.

Extended Data Fig. 3. Spike-specific T-cell responses (CD107a, IL-4, IL-10) in peripheral blood from convalescent and vaccinated patients. Comparison of the net frequency of $CD107a^+$ (left), IL-4^+ (middle), and IL-10^+ (right) cells within $CD4^+$ (upper) and $CD8^+$ (lower) T-cell subsets for each of the four groups after exposure of PBMCs to S-peptide pools. Data in bar graphs are shown as median ± IQR, where each dot represents an individual patient for each group (Ctrl, control, n=5; Inf, convalescent infected, n=9; Vx2, vaccine 2 doses, n=7 and Vx3, vaccine 3 doses, n=5). Statistical significance was determined by Kruskal-Wallis test (with Dunn´s post-test).

Extended Data Fig. 4. SARS-CoV-2-specific T-cell responses (CD107a, IL-4, IL-10) in the lung from convalescent and vaccinated patients. (**a**) Comparison of the net frequency of $CD107a^+$ (left), IL-4^+ (middle), and IL-10^+ (right) cells within $CD4^+$ (upper) and $CD8^+$ (lower) T-cell subsets for each of the four groups after exposure of single-cell suspensions of lung tissue to S-peptide pools. Data in bar graphs are shown as median ± IQR, where each dot represents an

individual patient for each group (Ctrl, control, n=5; Inf, convalescent infected, n=9; Vx2, vaccine 2 doses, n=7 and Vx3, vaccine 3 doses, n=5). Statistical significance was determined by Kruskal-Wallis test (with Dunn´s post-test). (**b**) Correlation between the net frequency of S-specific $CD107a^+$ cells of $CD4^+$ (left) and $CD8^+$ (right) T cells in the lung and age (Inf group). Correlations (*r* and *P* values) were assessed by Spearman test.

Extended Data Fig. 5. Comparison of the frequency of S-peptide specific $CD4^+$ and $CD8^+$ T cells between lung and blood. (**a-c**) Graphs show the individual patient net frequency of $CD107a^+$ (**a**), IL-4^+ (**b**), and IL-10^+ (**c**) cells within $CD4^+$ (left) and $CD8^+$ (right) T-cell subsets of paired blood and lung samples that were exposed to S-peptide pools. Statistical significance was determined using Friedmann test (with Dunn´s post-test) for the difference between blood and lung samples within each patient group.

Extended Data Fig. 6. The response of $CD4^+$ and $CD8^+$ (non-) T_{RM} cells against M and N peptide pools. (**a, b**) Comparison of the net frequency of IFNγ^+ cells within three T_{RM}-cell subsets of $CD4^+$ (left) and $CD8^+$ (right) T cells present in the lung: $CD69^-$ non-T_{RM}, $CD69^+$ T_{RM}, and $CD69^+CD103^+$ T_{RM} cells for each group after exposure to (**a**) M- and (**b**) N-peptide pools. Data in bar graphs are shown as median ± IQR, where each dot represents an individual patient for each group (Ctrl, control, n=5; Inf, convalescent infected, n=8; Vx2, vaccine 2 doses, n=7 and Vx3, vaccine 3 doses, n=4). Statistical significance was determined using Friedmann test (with Dunn´s post-test) for the difference between the cellular subsets within each patient group. (**c**) Correlation between the net frequency of lung S-specific IFNγ^+ cells within the $CD8^+$ $CD69^+$ $CD103^+$ T_{RM} subset and days since confirmed infection and sampling (Inf group). (**d**) Correlation between the net frequency of S-specific $CD107a^+$ $CD8^+$ $CD69^+$ $CD103^+$ T_{RM} cells or $CD8^+$ $CD69^+$ T_{RM} cells and age (Inf group). Correlations (*r* and *P* values) were assessed by Spearman test.

Extended Data Fig. 7. Frequency of polyfunctional T-cell responses against spike with a tissue-resident phenotype in the lung. Comparison of the net frequency of S-specific polyfunctional $CD107a^+$ IFNγ^+ cells within lung $CD4^+$ (upper) and $CD8^+$ (lower) (non-) tissue-resident cell subsets ($CD69^-$ non-T_{RM}, $CD69^+$ T_{RM}, and $CD69^+CD103^+$ T_{RM} cells) for each of the four patient groups after exposure of single-cell lung suspensions to S-peptide pools. Data in bar graphs are shown as median ± IQR, where each dot represents an individual patient for each group (Ctrl, control, n=5; Inf, convalescent infected, n=8; Vx2, vaccine 2 doses, n=7 and Vx3,

vaccine 3 doses, n=4). Statistical significance was determined by Kruskal-Wallis test (with Dunn´s post-test) for the difference between the groups.

Extended Data Fig. 8. T-cell responses for patient #174. (**a**) Timeline for patient 174, indicating vaccination against SARS-CoV-2, infection with SARS-CoV-2, and acquisition of blood and lung samples. (**b**) Donut charts displaying the net contribution of each functional marker (IFNγ, CD107a, IL-4, IL-10, or no response) to the M-, N-, and S-specific $CD4^+$ and $CD8^+$ T-cell response within the lung resident and non-resident T-cell subsets and in peripheral blood for patient 174. The frequency shown inside each donut chart represents the accumulated mean response of all functions. (**c**) Flow-cytometry plots of patient 174 showing $CD4^+$ (upper) and $CD8^+$ (lower) T cells expressing CD107a and IFNγ after exposure of lung single-cell suspensions (left) and PBMCs (right) to M-, N- and S-peptide pools or left unstimulated.

Extended Data Fig. 9. T-cell responses for patient #162, longitudinal samples. (**a**) Timeline for patient 162 who was longitudinally sampled, first ~4 months after SARS-CoV-2 infection and then ~1 month after third dose mRNA-vaccination. (**b, c**) Donut charts displaying the net contribution of each functional marker (IFNγ, CD107a, IL-4, IL-10, or no response) to the M-, N-, and S-specific $CD4^+$ and $CD8^+$ T-cell response within the lung resident and non-resident T-cell subsets and in peripheral blood for patient 162 in the first sample (**b**) and second sample (**c**). The frequency shown inside the donut chart represents the accumulated mean response of all functions.

Extended Data Fig. 10. Longitudinal patterns of SARS-CoV-2-specific T-cell responses in lung and blood for patient #162. (**a, b**) Flow-cytometry plots showing longitudinal data (left, after infection, sample 1; right, after third-dose vaccination, sample 2) of patient 162 showing $CD4^+$ (top) and $CD8^+$ (bottom) T cells expressing CD107a and IFNγ after exposure of PBMCs (**a**) and lung cell suspension (**b**) to M-, N-, and S-peptide pools or left unstimulated (vehicle).

Extended Table 1. Patient characteristics

	Control n=5	**Infected** n=9‡	**Vx2** n=7‡	**Vx3** n=5‡	***P* value between groups**
Age (Years), median [IQR]	**67** [66-74]	**69** [65-71]	**61** [58-70]	**72** [69-73]	0.6555[a]
Female, n (%)	**1/5** (20%)	**1/9** (11%)	**4/7** (57%)	**3/5** (60%)	0.0875[b]
Days after infection* or vaccination, median [IQR]	N/A	**304** [183-320]	**206** [184-234]	**52** [42-54]	**0.0006[a]**
Spike-specific IgG** (AU/mL), median [IQR] (AU/mL)	**<1.85** [1.85-1.85]	**133.1** [89.04-228.46]	**225** [118.85-248.46]	**800** [716,35-800]	**0.0122[a]**
Total nucleocapsid-specific Ig** (Index), median [IQR]	**0.07** [0.07-0.08]	**135** [62.1-157.5]	**0.1** [0.07-0.11]	**0.1** [0.06-0.09]	**0.0001[a]**
Virus neutralization titer***, median [IQR]	**0** [0-0]	**40** [19-56]	**50** [46.25-471.5]	**138.5** [67.75-665.75]	0.0974[a]
Patients with SARS-CoV-2 neutralization capacity, n (%)	**0/5** (0%)	**5/7** (71%)	**5/6** (83%)	**4/4** (100%)	0.4877[b]
New infection after sampling, n (%)	**0/5** (0%)	**0/9** (0%)	**1/7** (14%)	**0/5** (0%)	0.3763[b]

* Confirmed by RT-PCR for SARS-CoV-2

** Measured by anti-SARS-CoV-2 S and N immunoassay

*** Measured by SARS-CoV-2 neutralization assay

‡ Plasma samples were not available for every patient

N/A not available

[a] Kruskal-Wallis test with Dunn's post-test

[b] Chi-square test

Figure 1

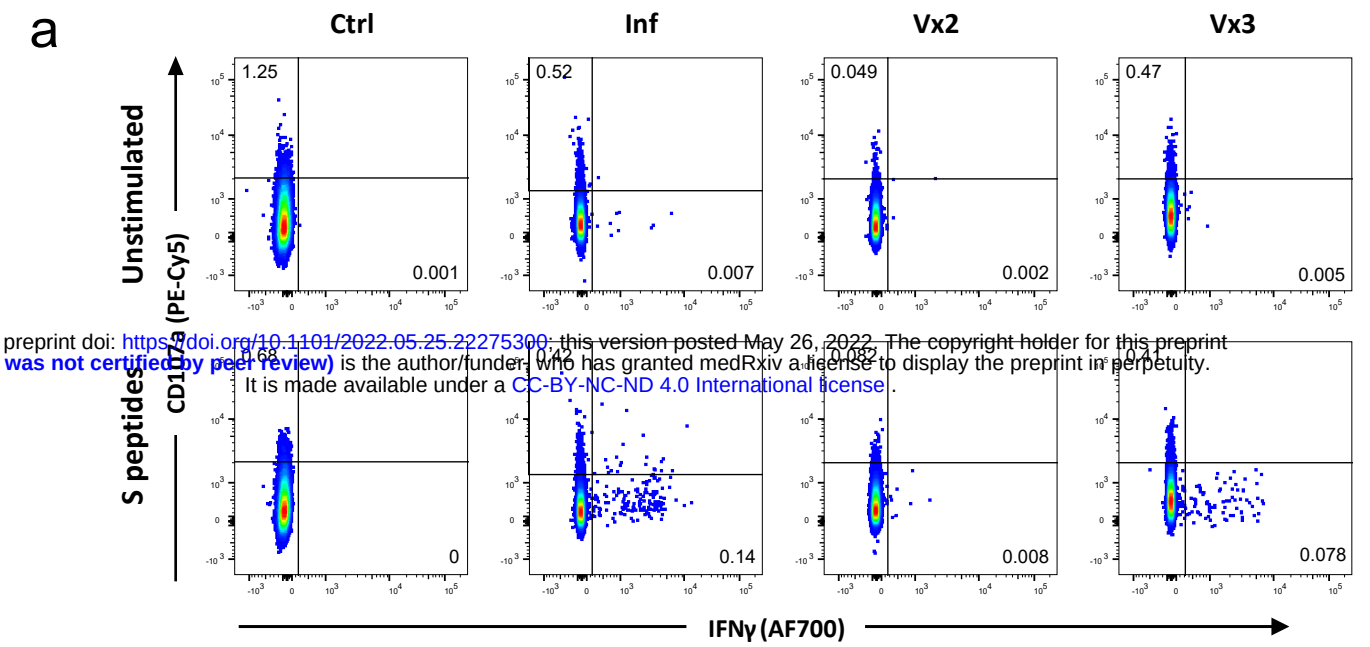

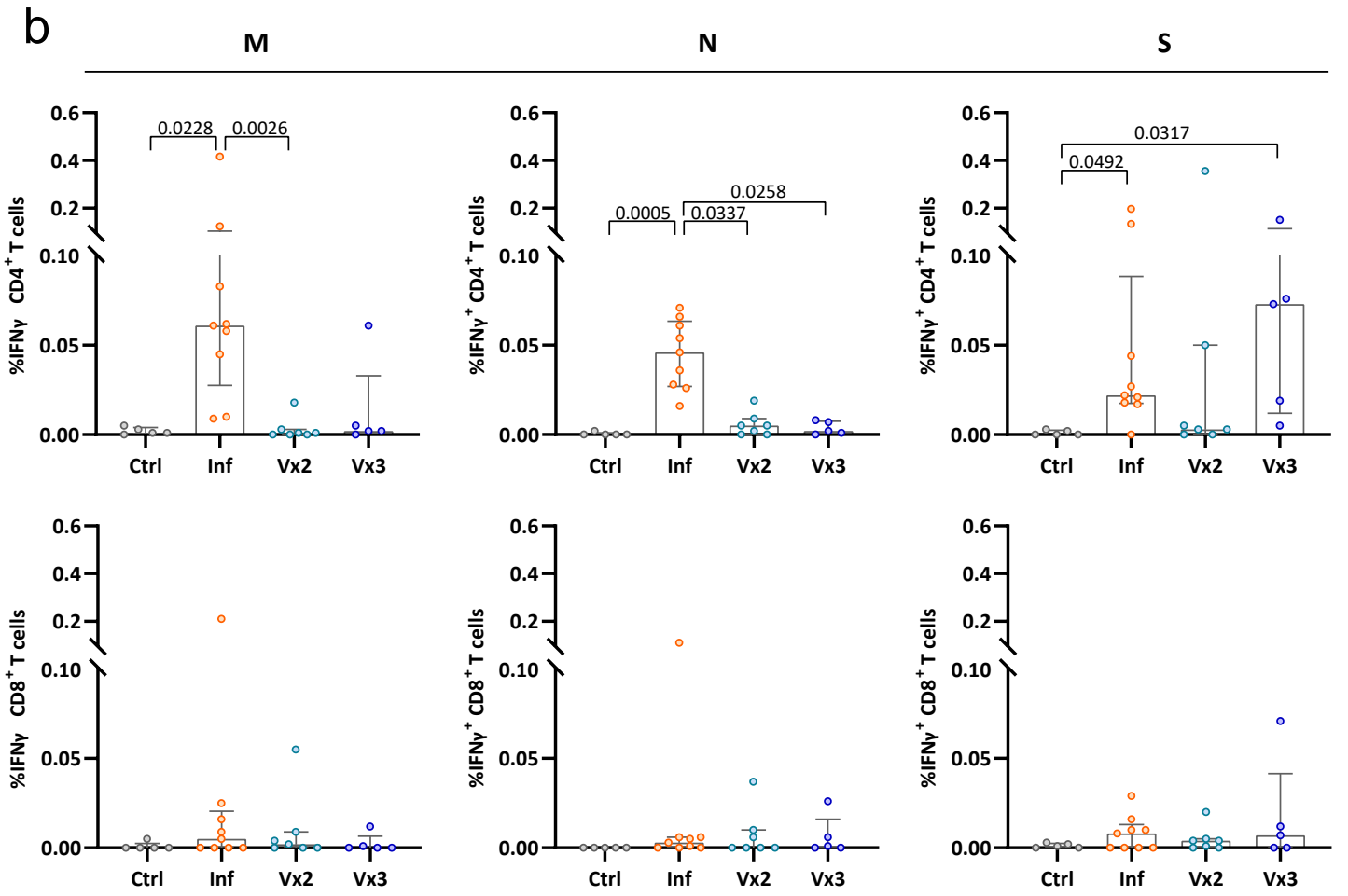

Figure 2

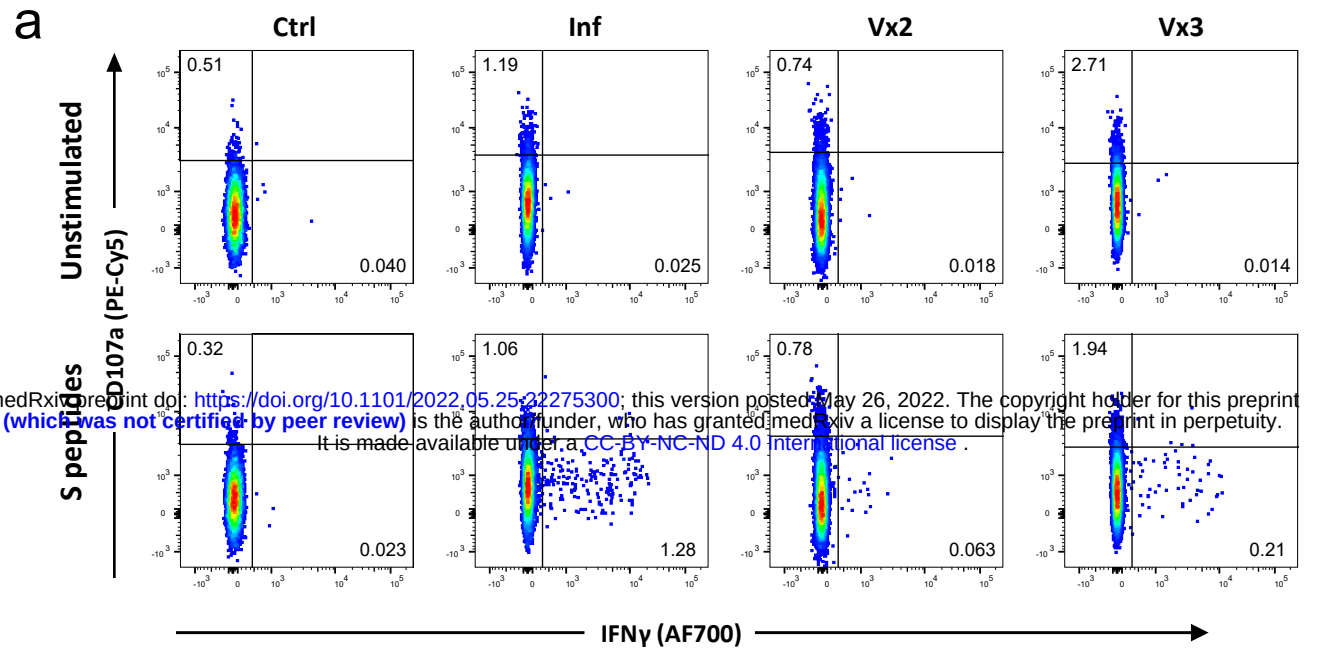

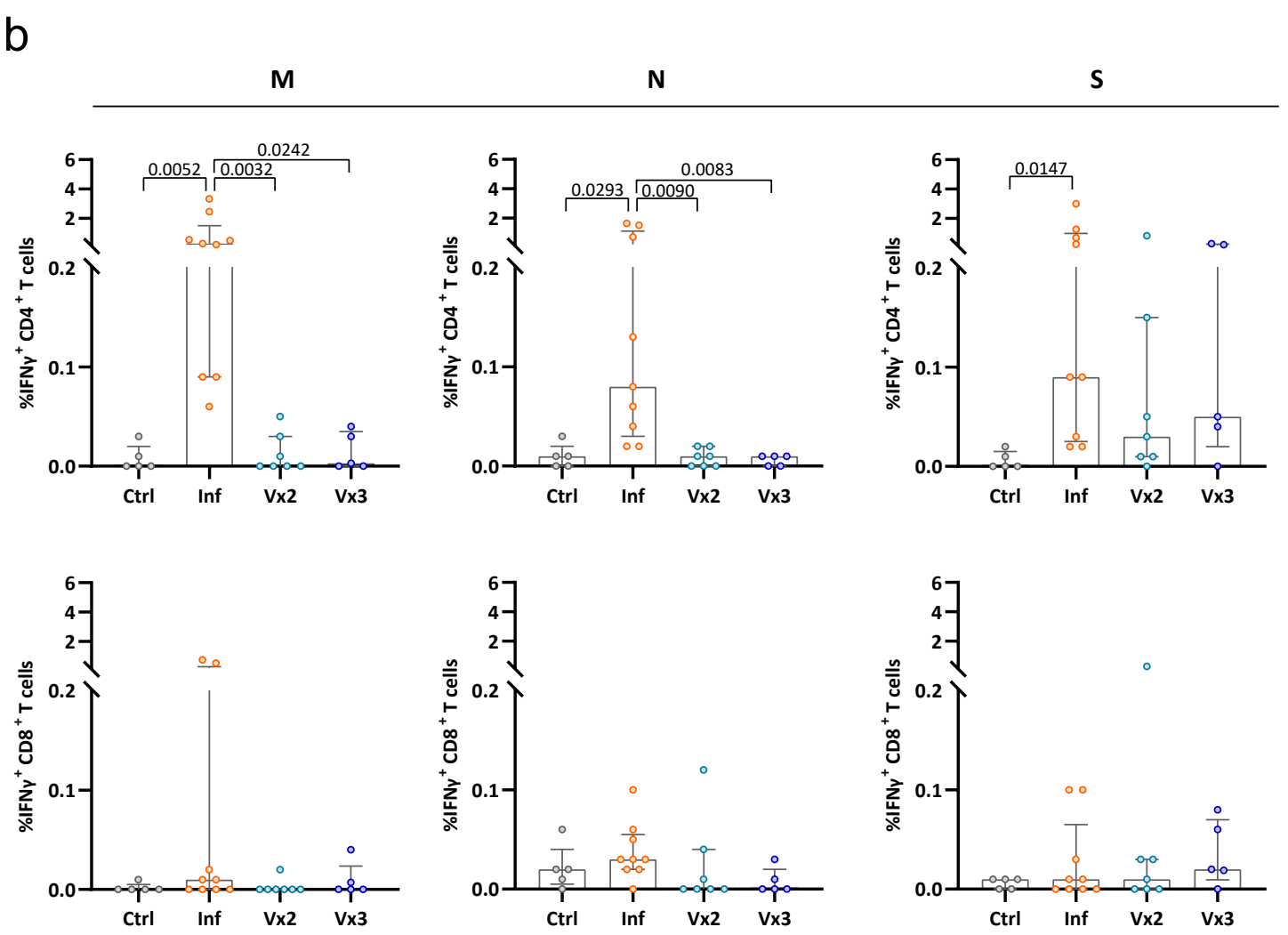

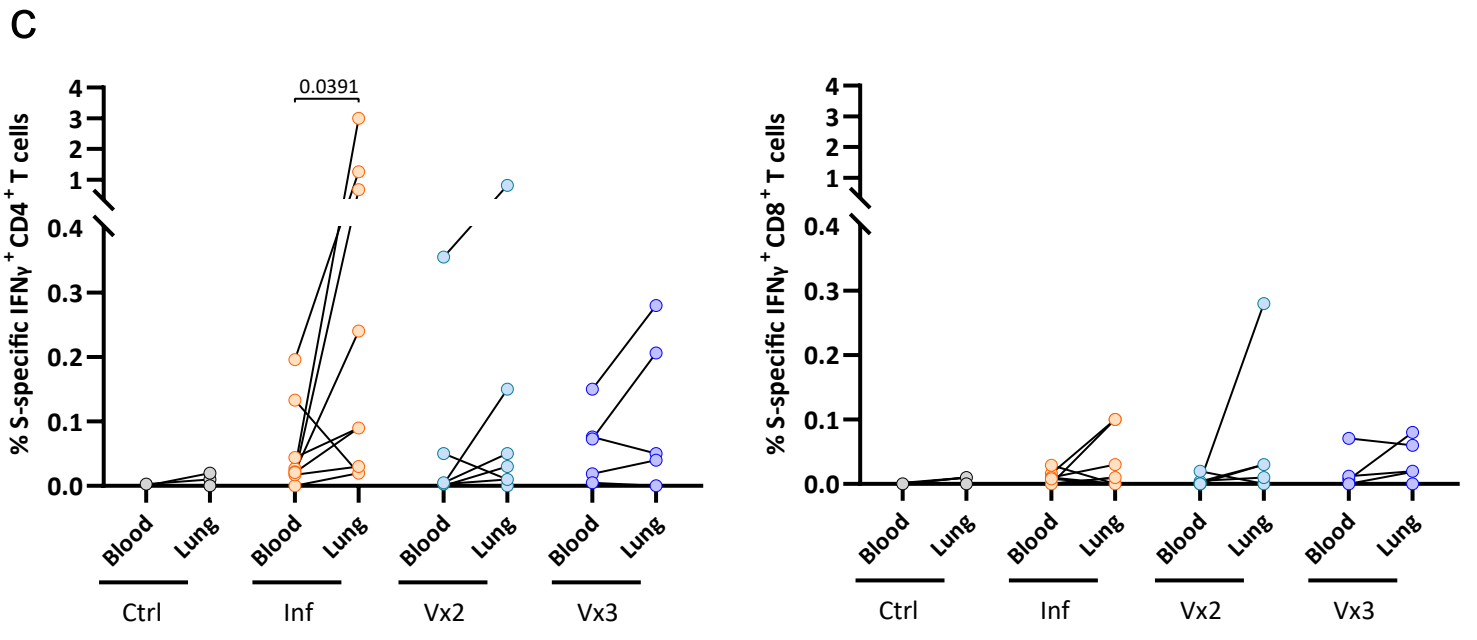

a

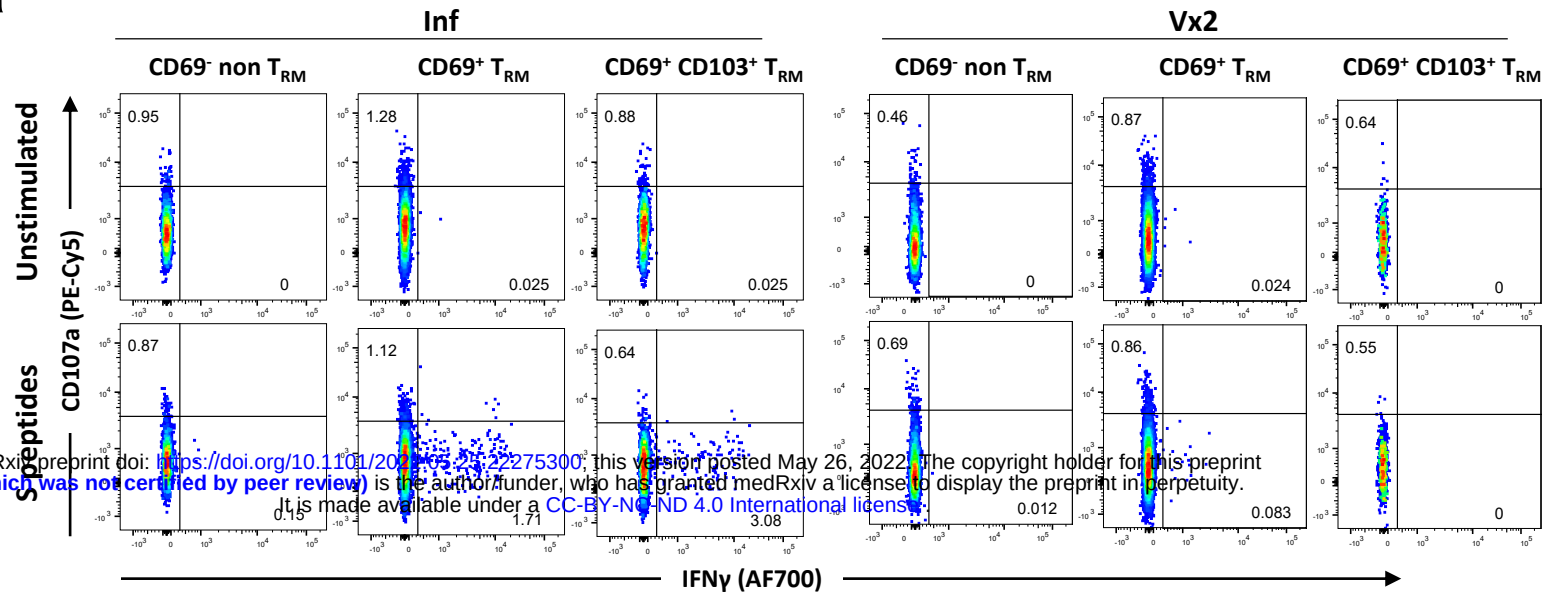

b

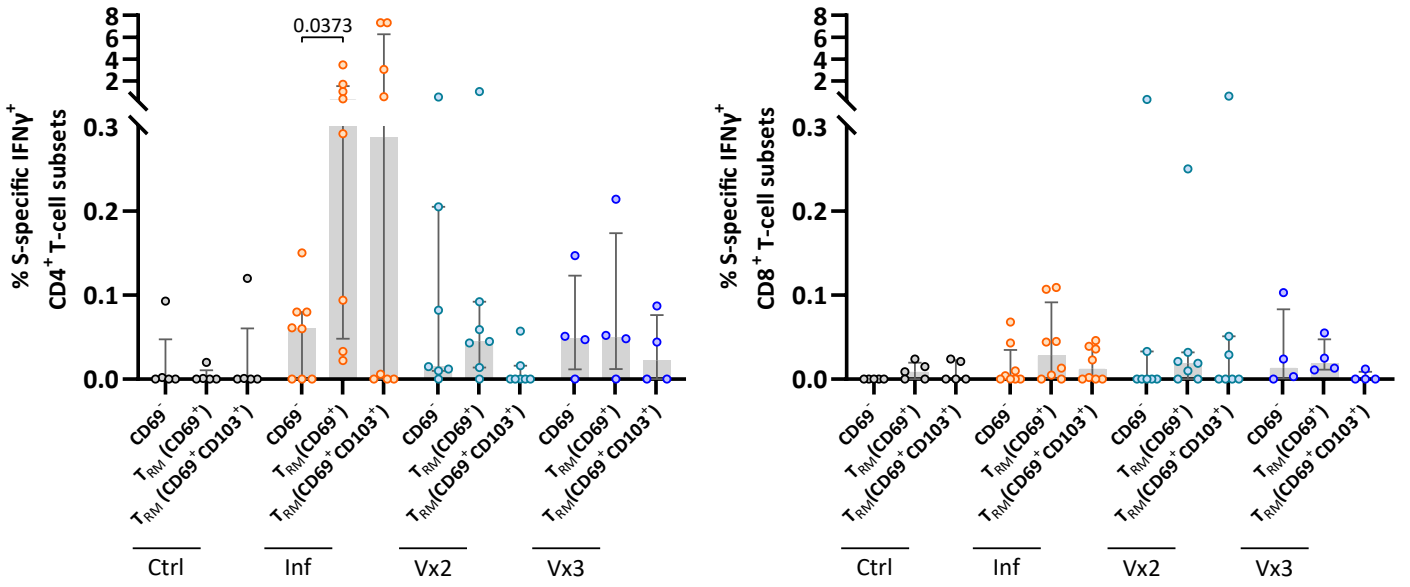

a

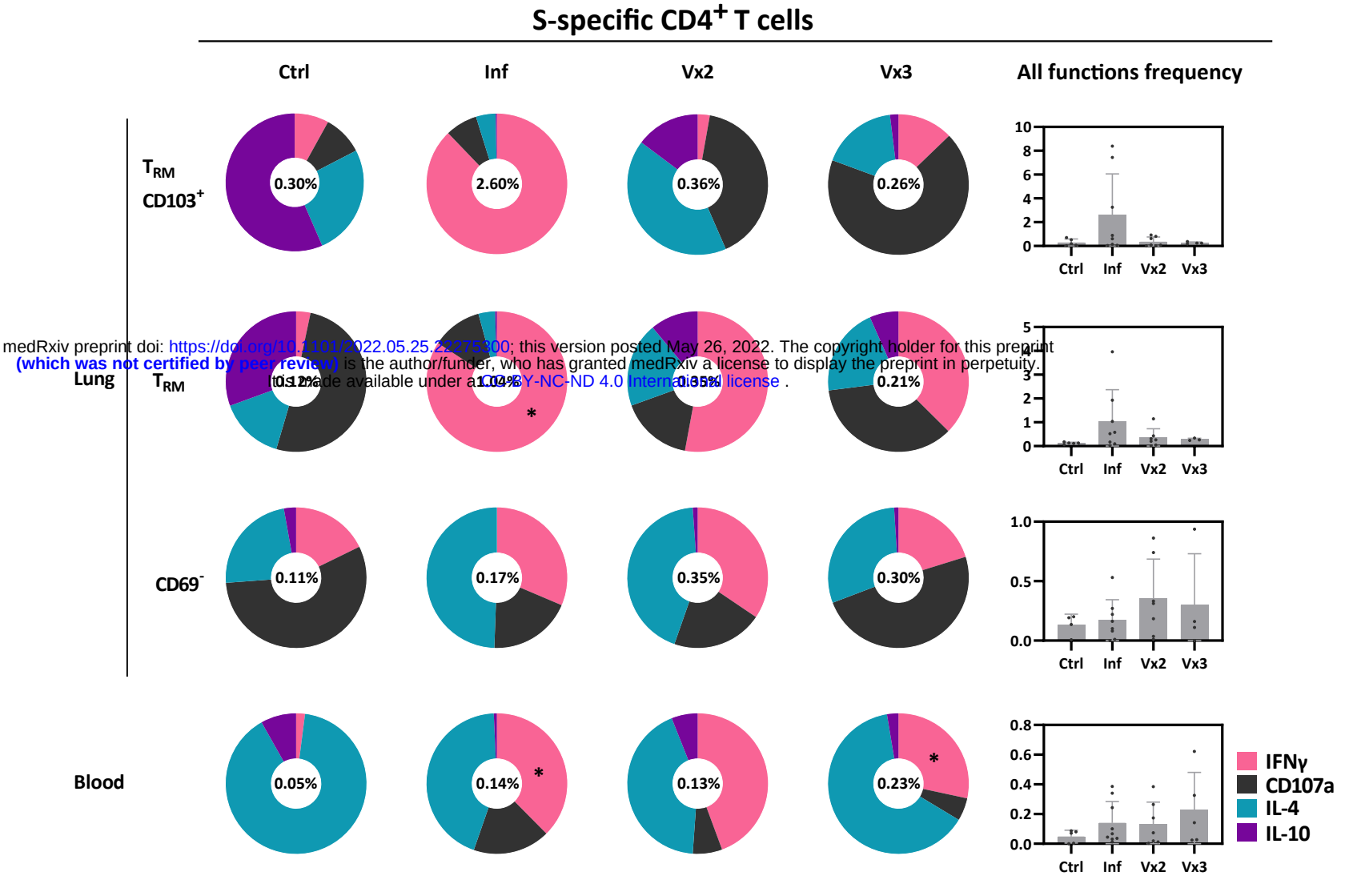

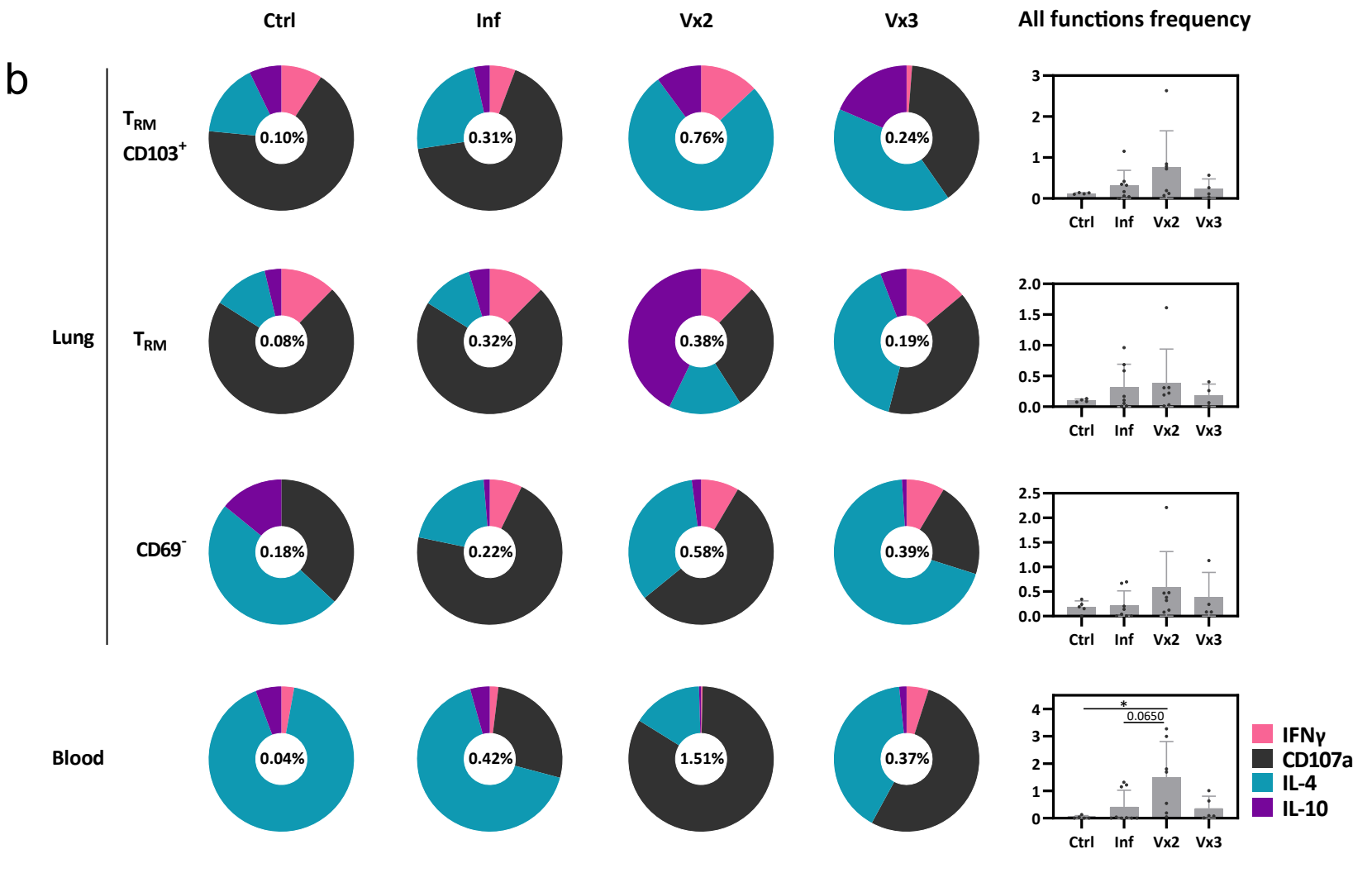

a

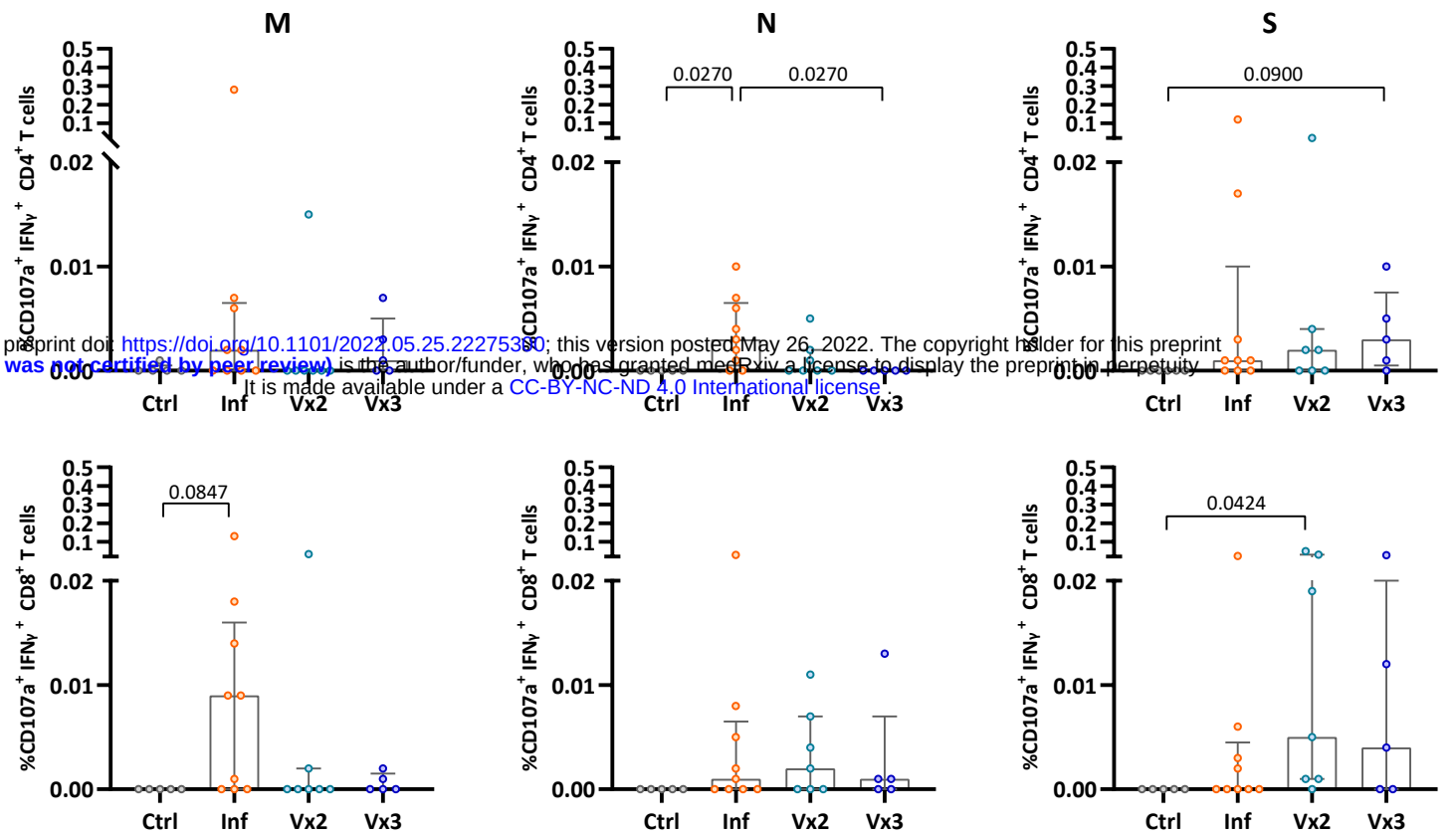

b

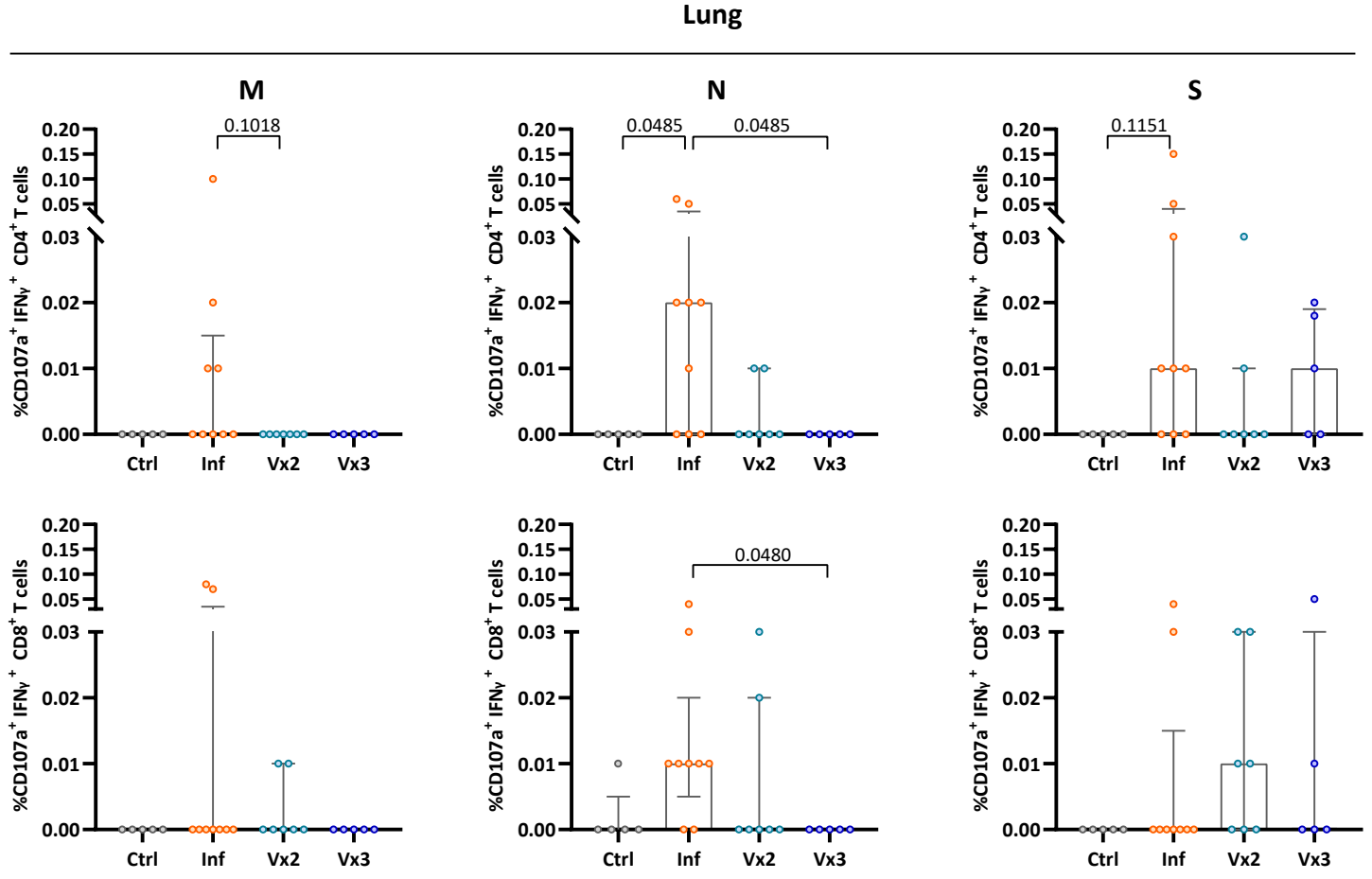

Extended Figure 1

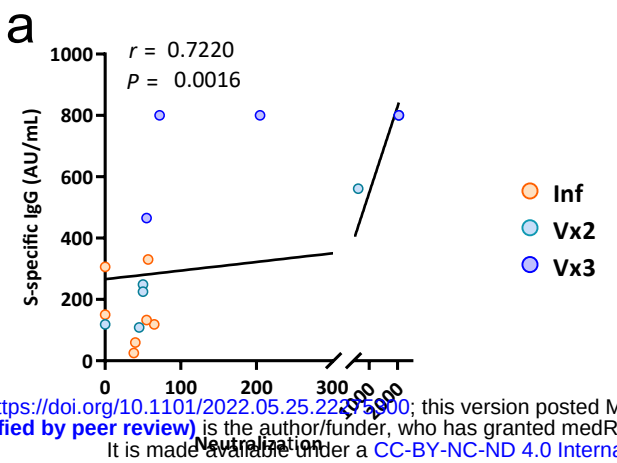

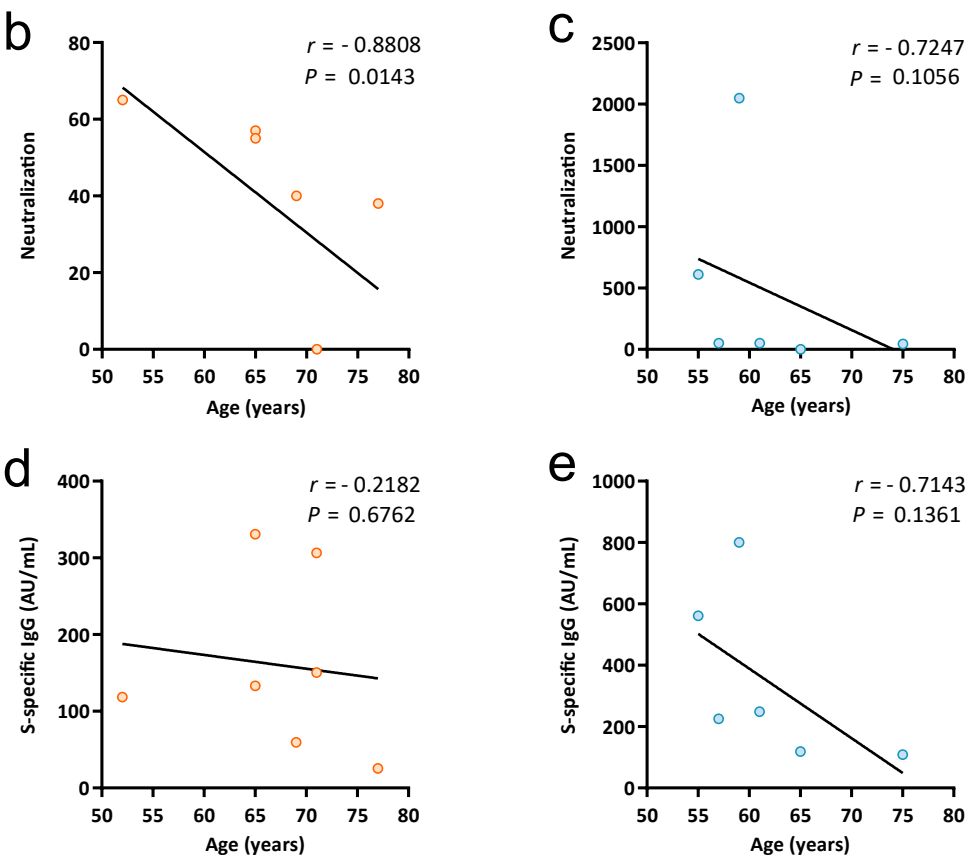

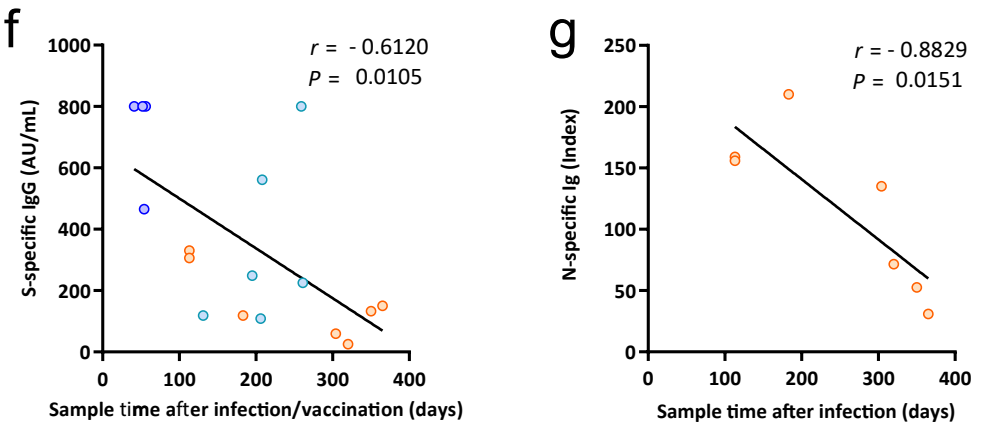

Extended Figure 2

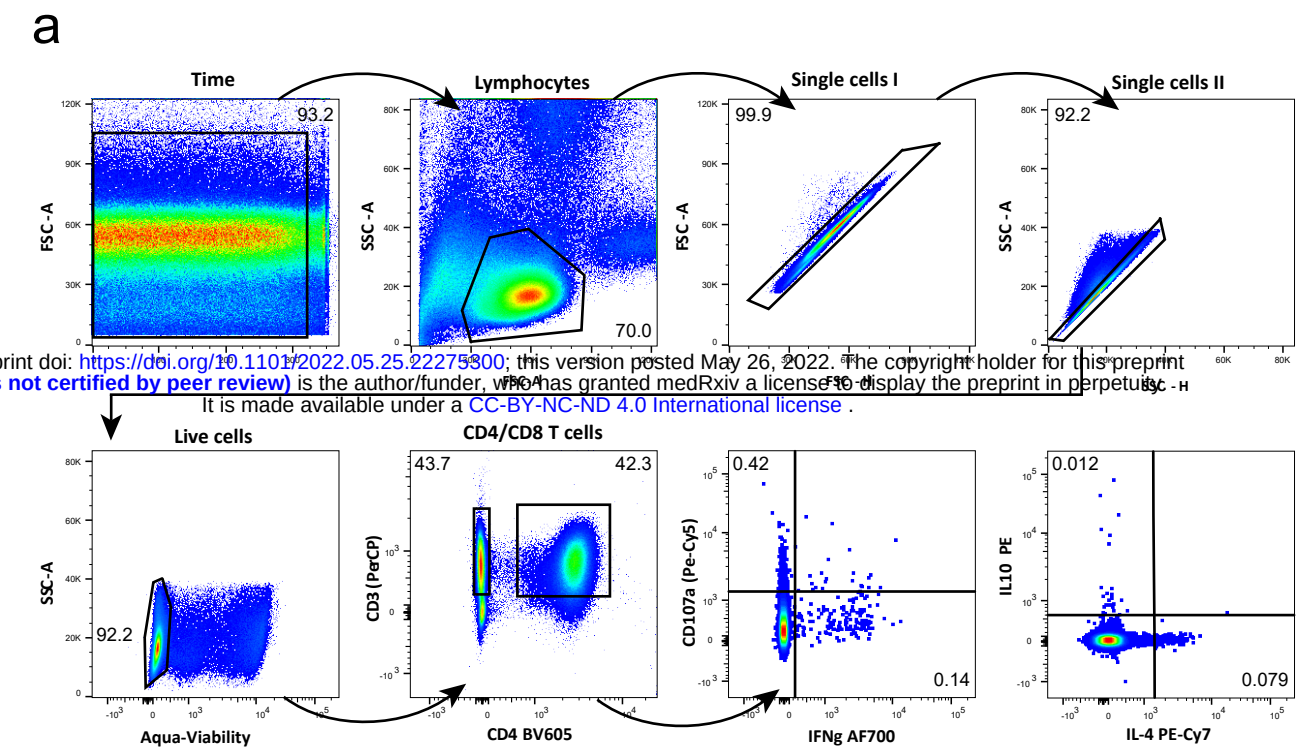

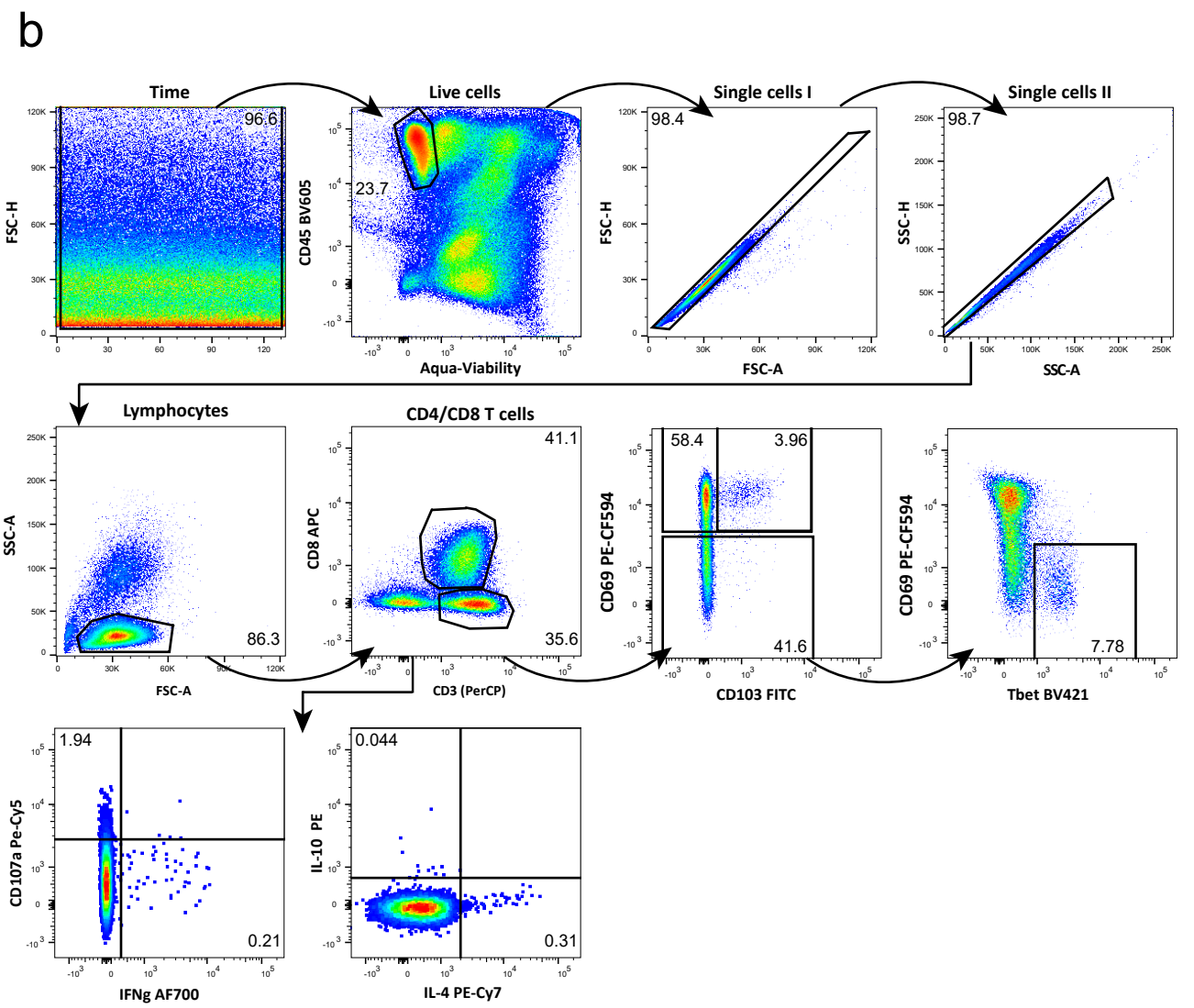

Extended Figure 3

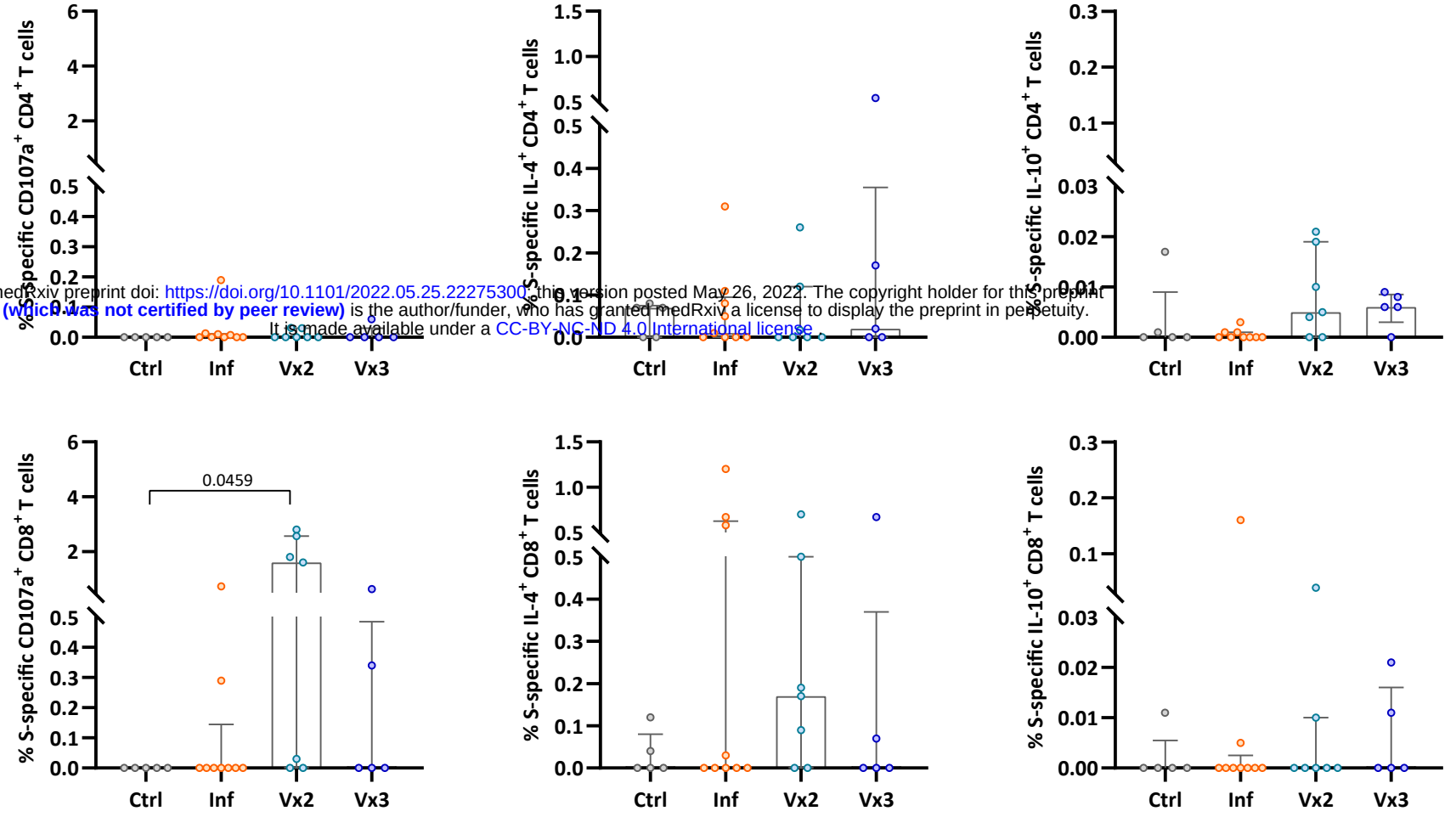

Extended Figure 4

a

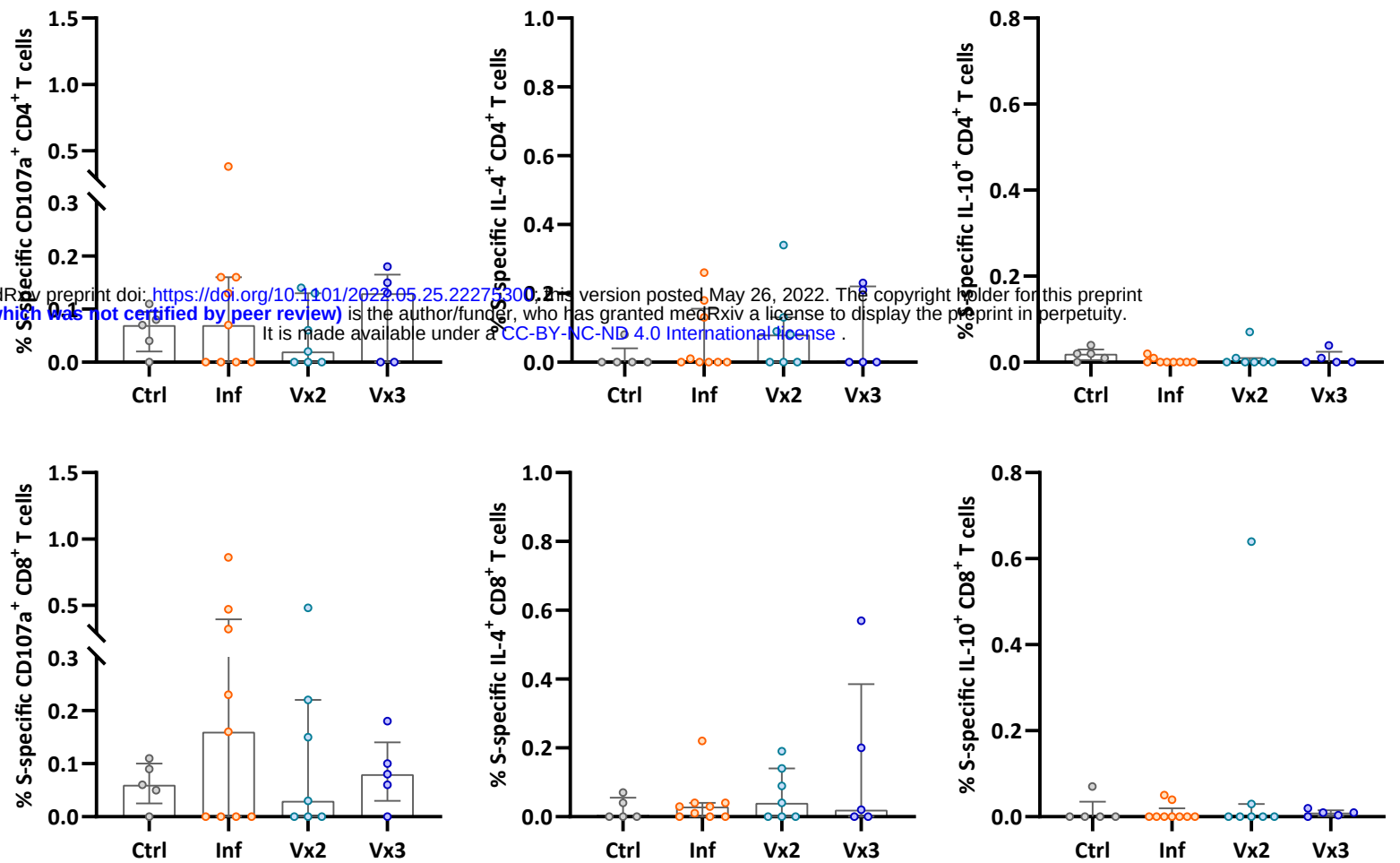

b

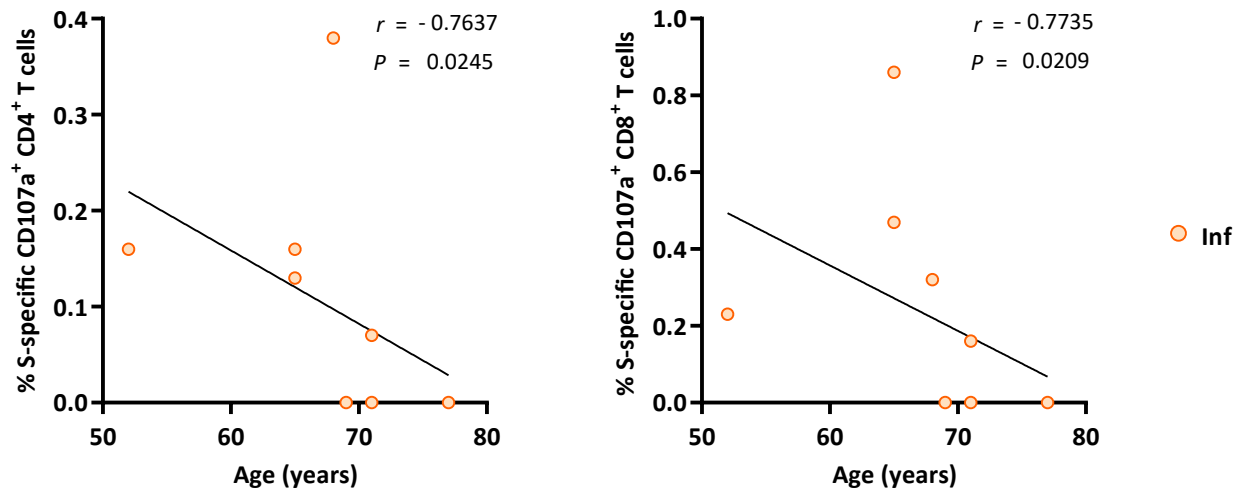

Extended Figure 5

a

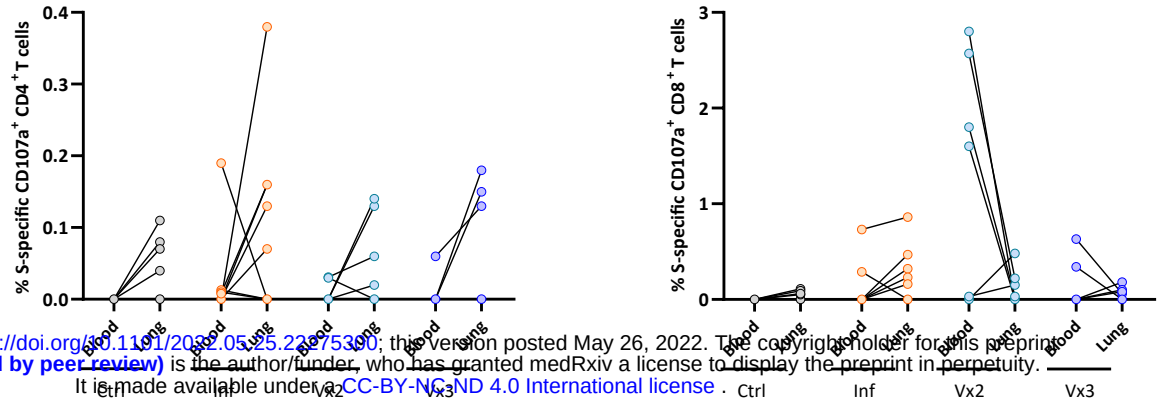

b

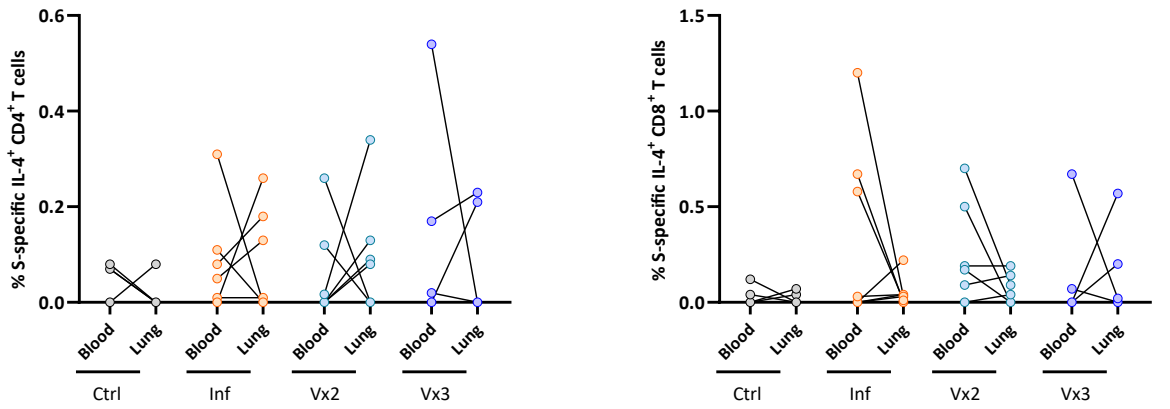

c

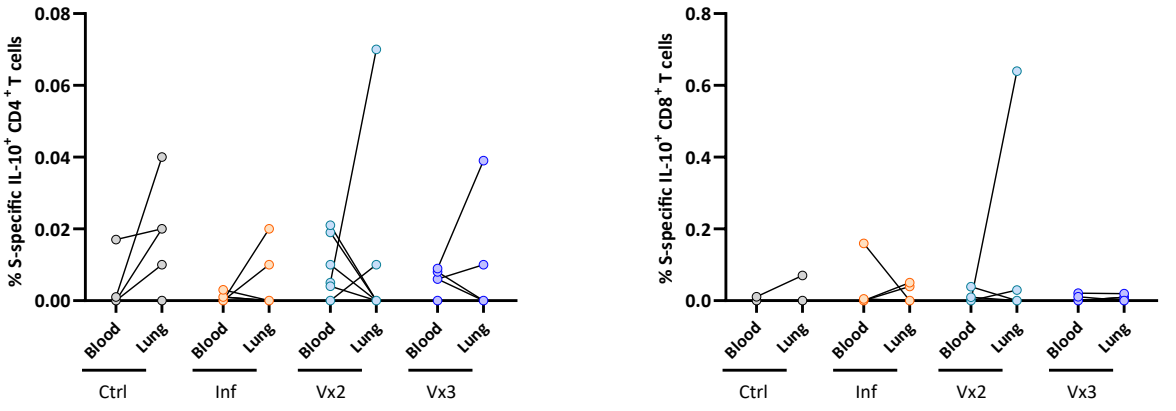

Extended Figure 6

a

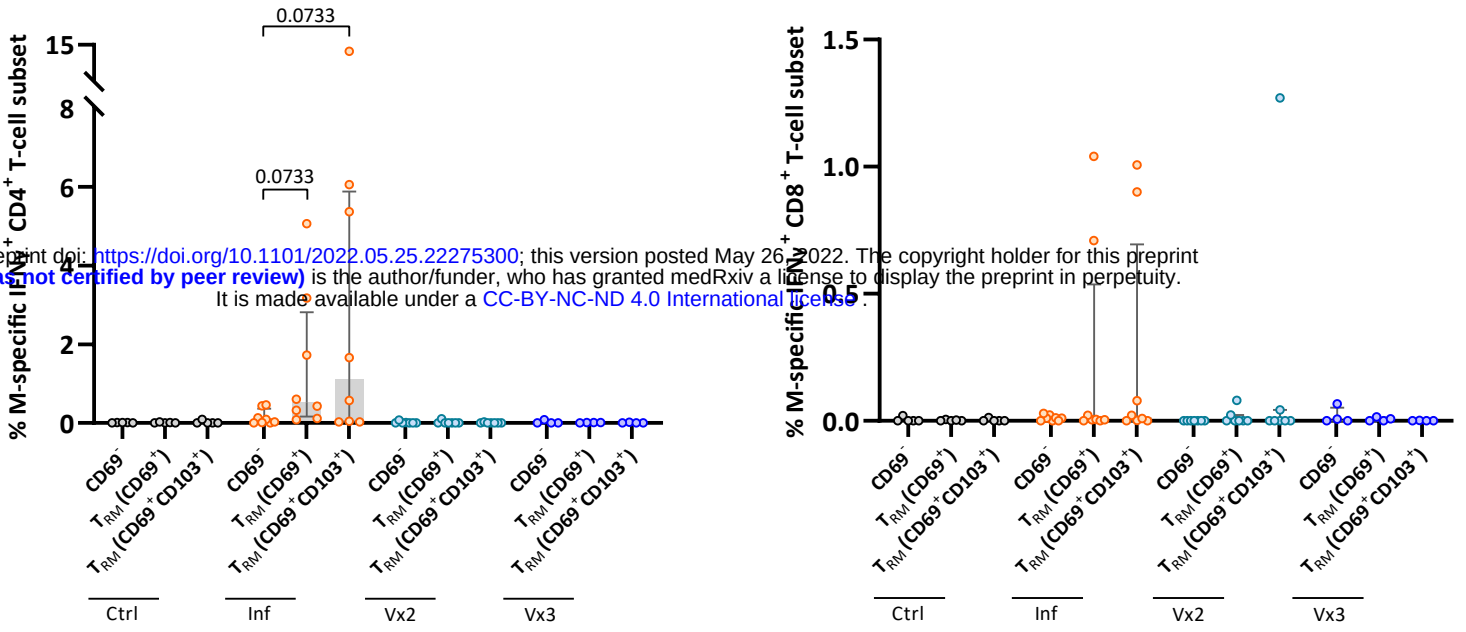

b

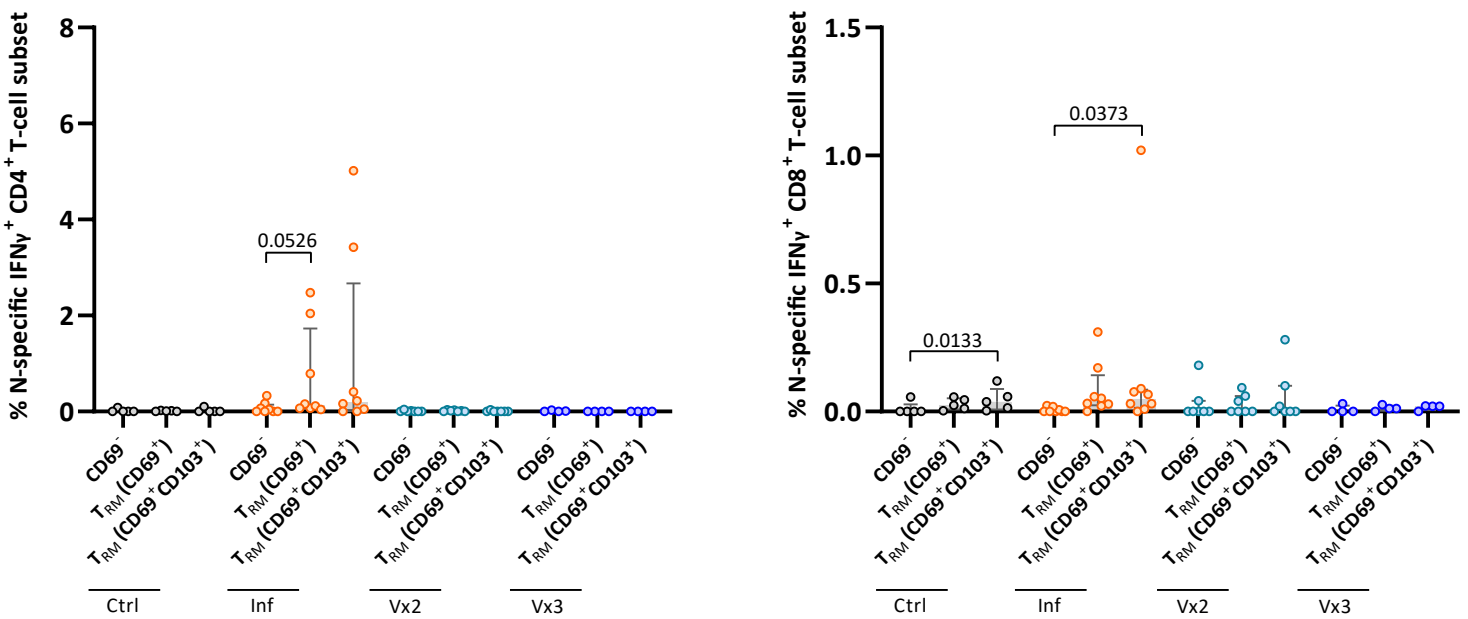

c

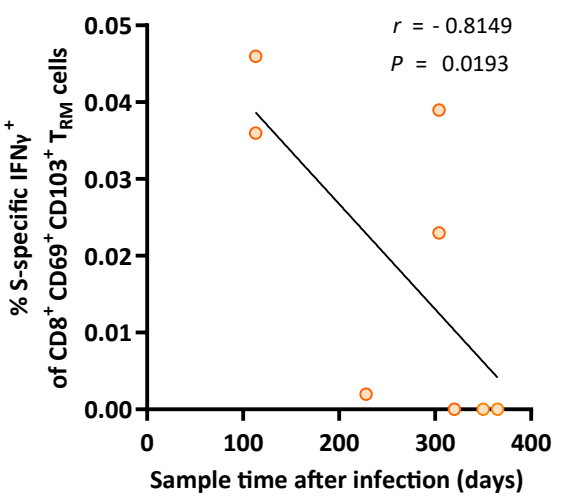

d

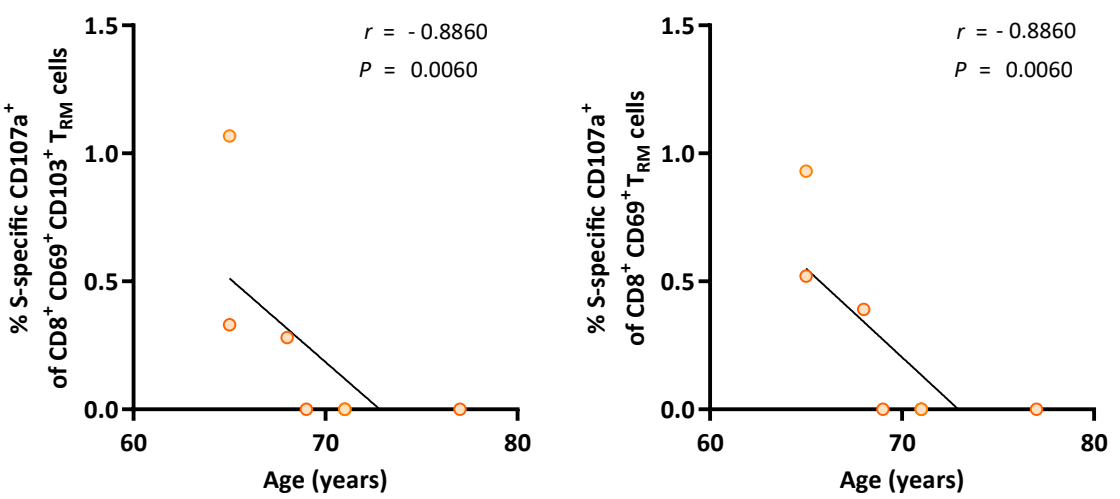

Extended Figure 7

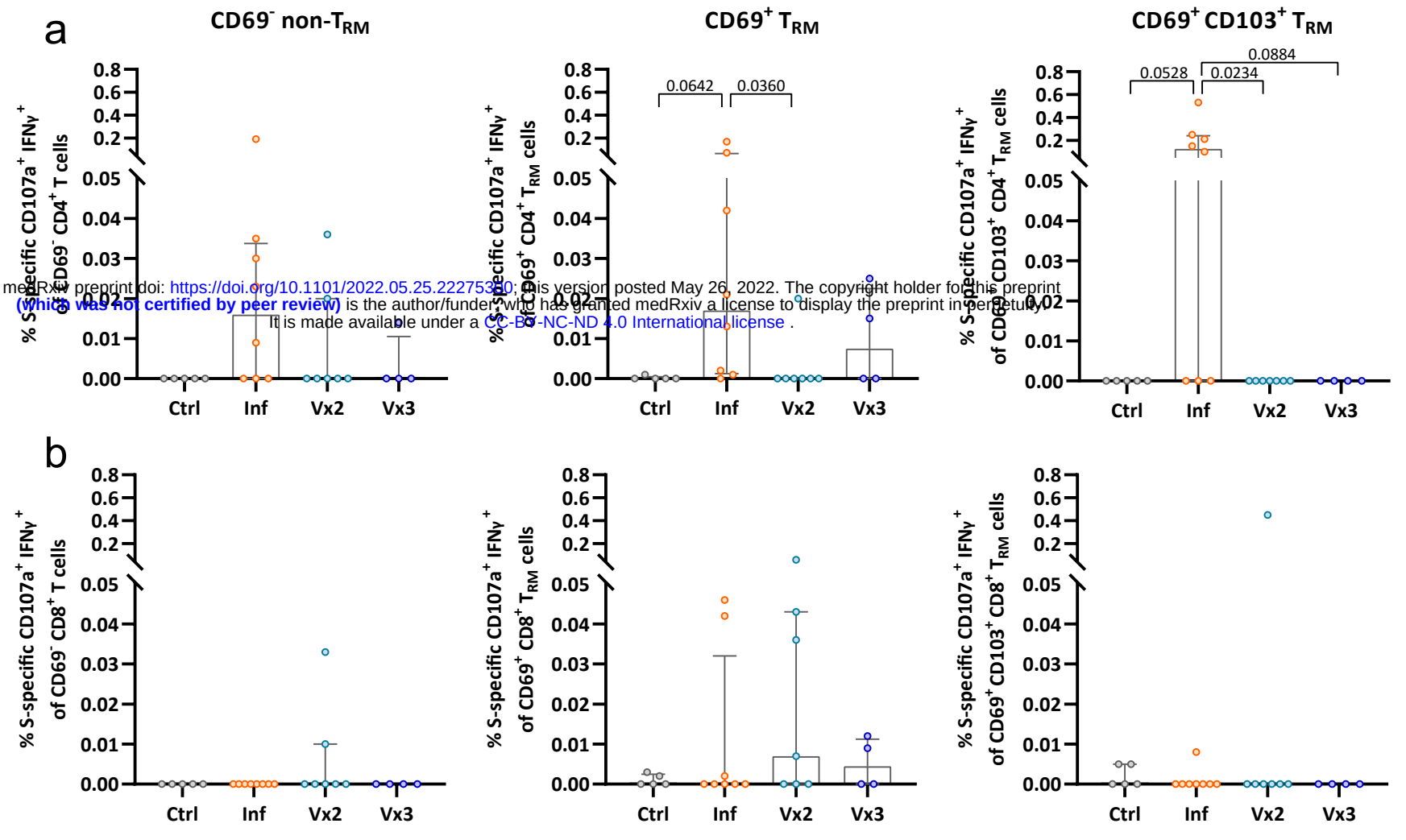

Extended Figure 8

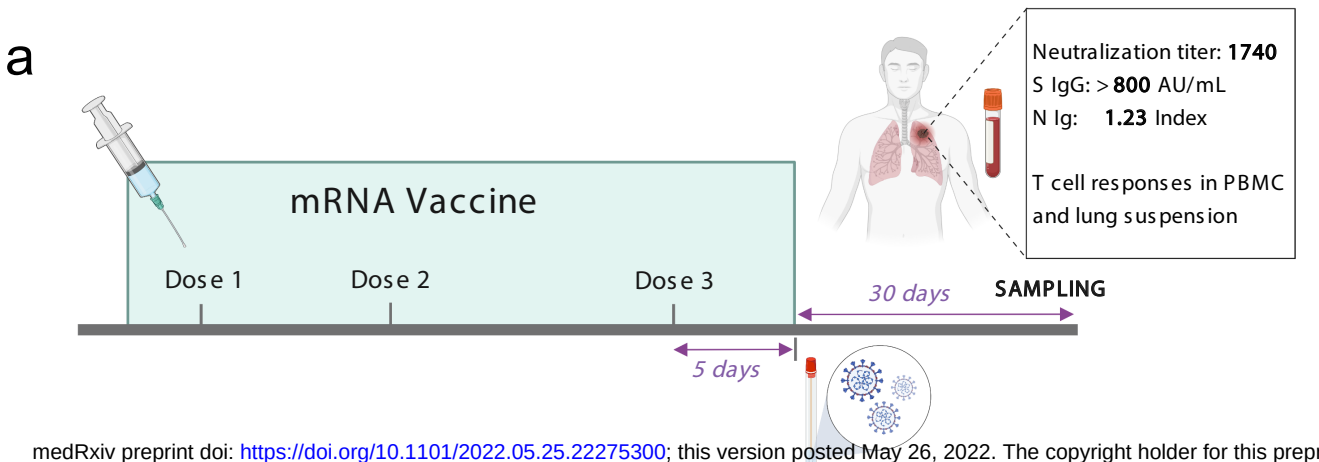

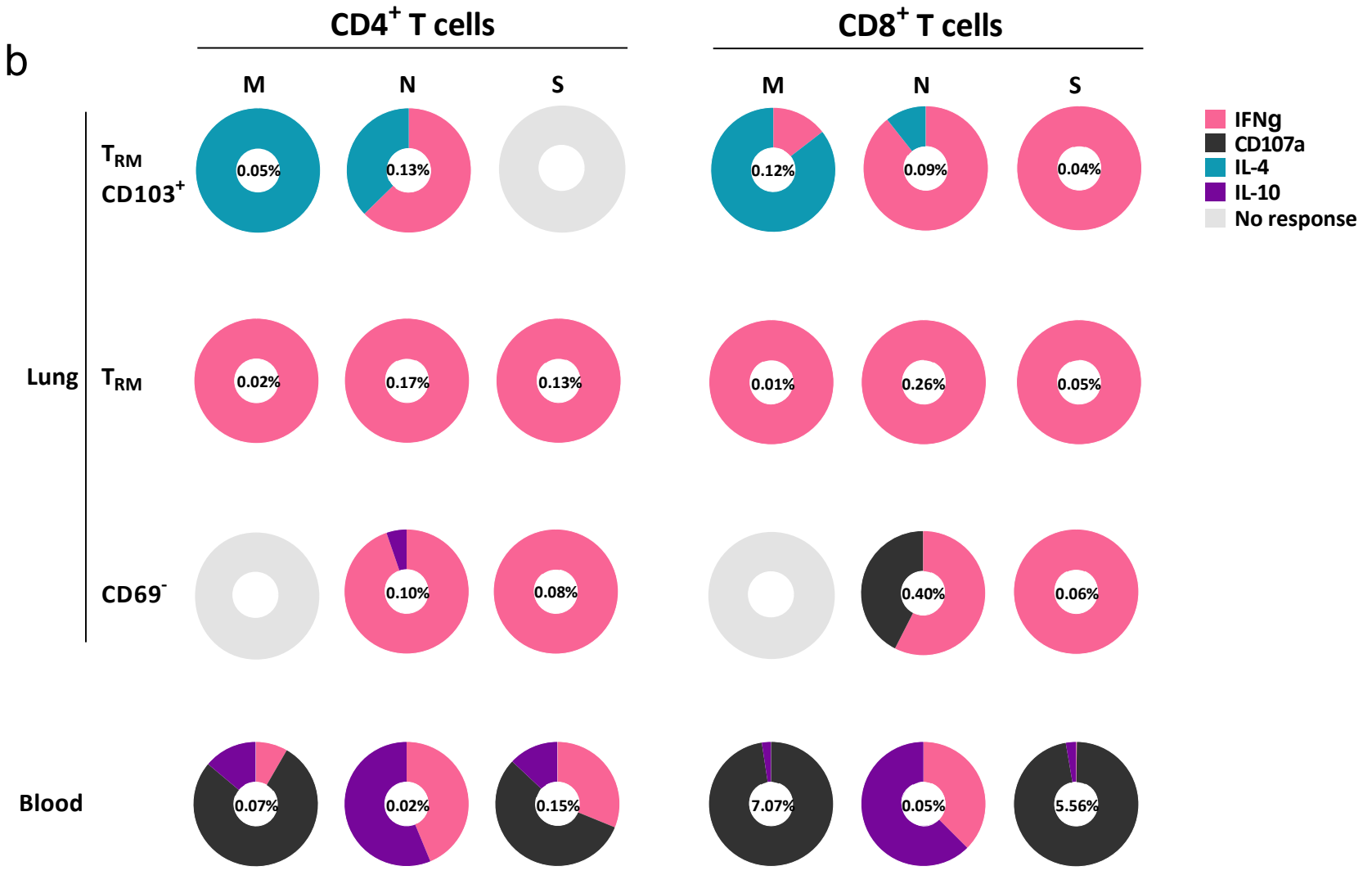

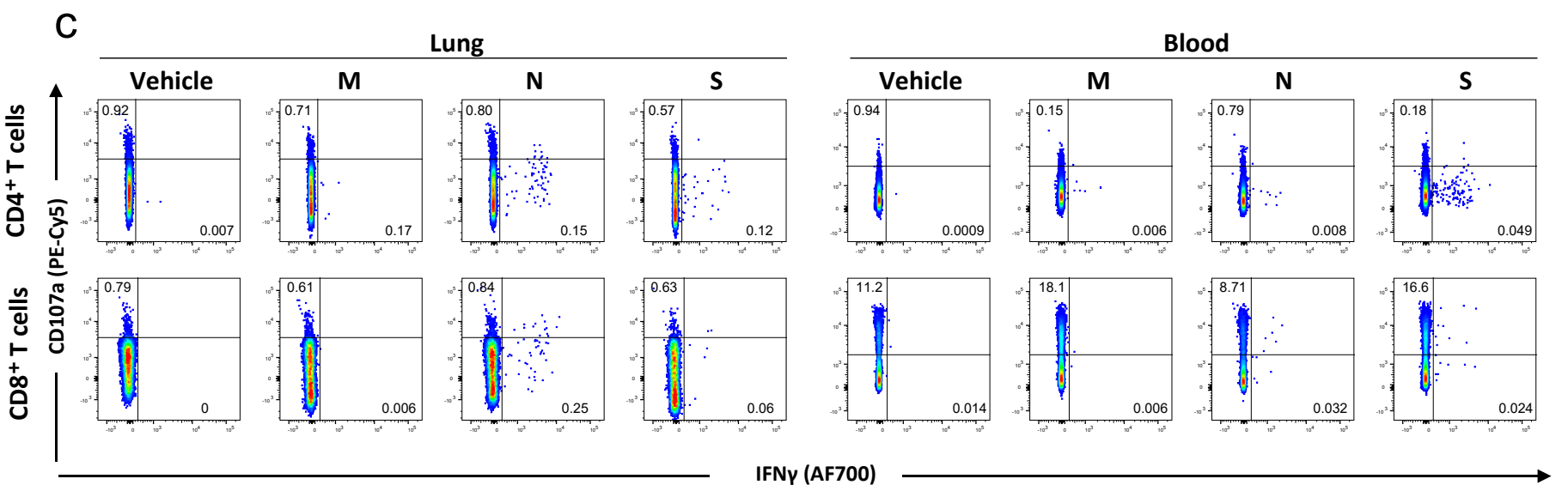

Extended Figure 9

a

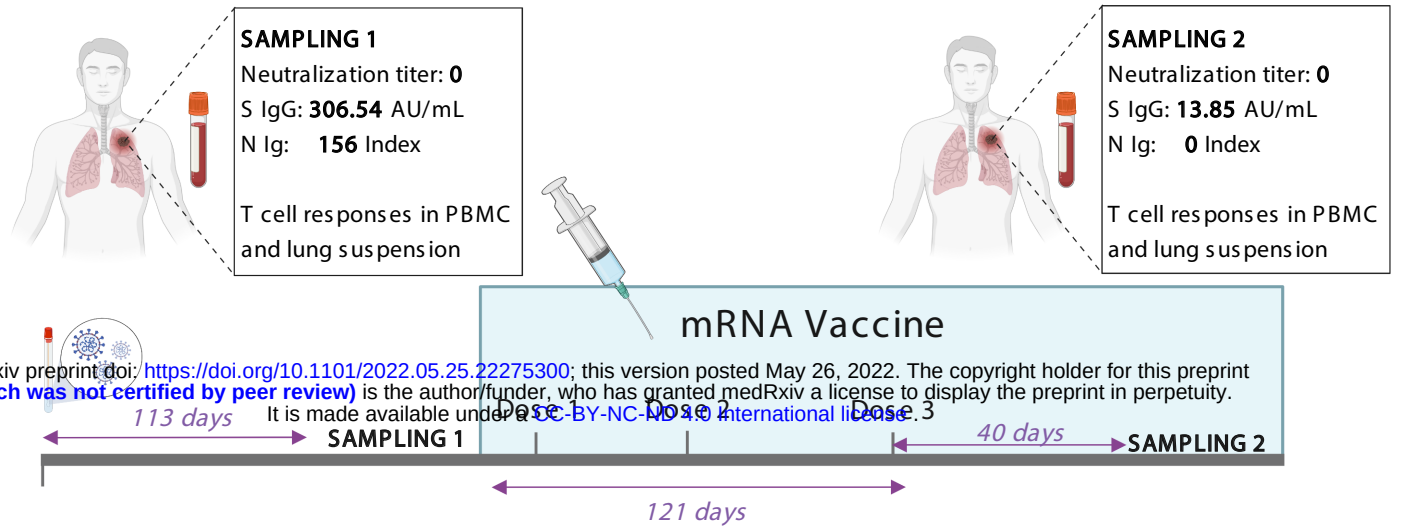

b

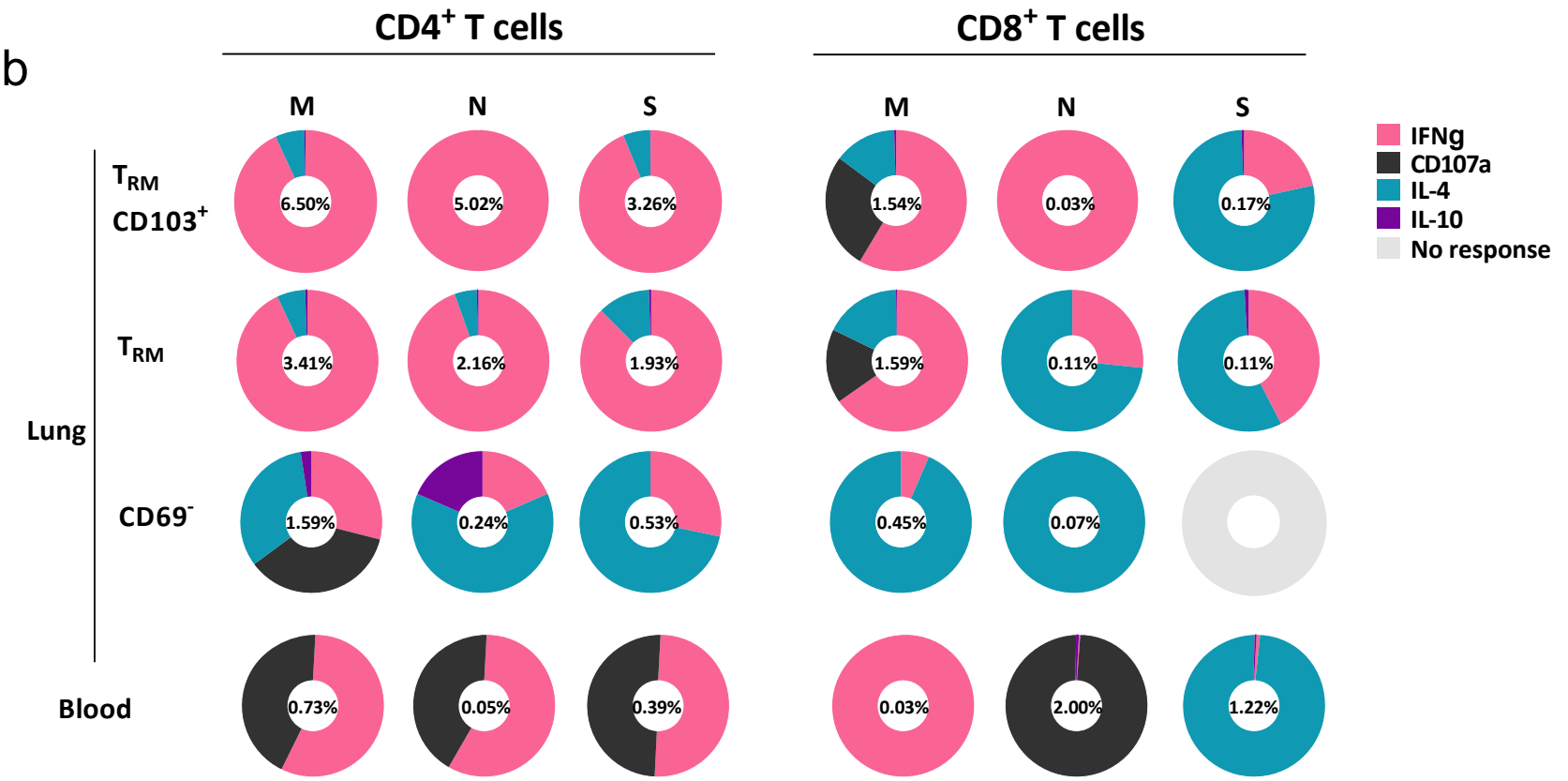

C

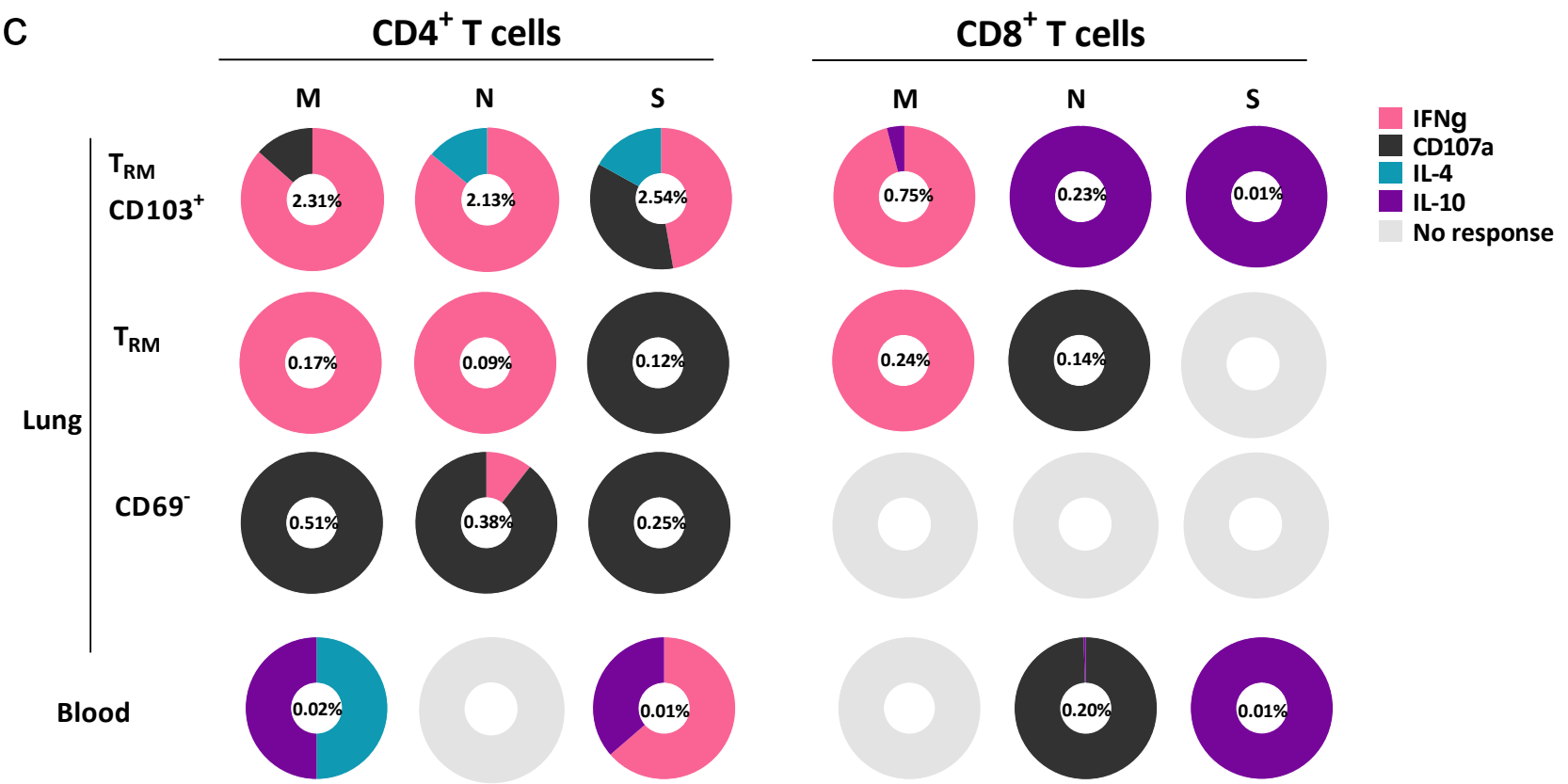

Extended Figure 10